


 Cite this: *RSC Adv.*, 2026, 16, 5353

# Photocatalytic degradation of dyes by metal sulfide–chitosan based composites: a comprehensive review

 Muhammad Arif \*

The growing prevalence of synthetic dyes in aquatic environments has intensified the search for sustainable and efficient photocatalytic remediation technologies. Metal sulfide (MS) photocatalysts have attracted considerable interest owing to their strong visible-light absorption and tunable electronic structures. However, their practical application is constrained by rapid charge recombination and photo-corrosion. This review uniquely positions metal sulfide–chitosan (MS–CS) composites as a next-generation solution by critically elucidating the synergistic interplay between the functional groups of chitosan (CS) and metal sulfide band structures that remain insufficiently addressed in existing literature. Unlike conventional polymer–semiconductor systems, chitosan not only enhances dye adsorption and nanoparticle stability but also actively regulates interfacial charge transfer and reactive oxygen species (ROS) generation. This review systematically analyzes photocatalytic mechanisms, structure–property relationships, heterojunction engineering, and performance of MS–CS composites under different environments, while identifying key design parameters governing performance under realistic conditions. By integrating material chemistry with mechanistic insights and application-oriented perspectives, this work bridges current knowledge gaps and establishes MS–CS composites as a viable and sustainable platform for advanced wastewater treatment.

 Received 11th October 2025  
 Accepted 30th December 2025

DOI: 10.1039/d5ra07777j

[rsc.li/rsc-advances](https://rsc.li/rsc-advances)

Department of Chemistry, School of Science, University of Management and Technology, Lahore 54770, Pakistan. E-mail: Muhammadarif2861@yahoo.com; Muhammadarif@umt.edu.pk


**Muhammad Arif**

*Dr Muhammad Arif has been a Professor (Assistant) in Chemistry at the Department of Chemistry, University of Management and Technology, Lahore since 2022. He worked as a lecturer in Chemistry at the Department of Chemistry, School of Science, University of Management and Technology, Lahore from 2017 to 2022. He has a PhD in Chemistry from the University of The Punjab, Lahore, Pakistan. He obtained his MPhil*

*in Chemistry and MSc in Organic Chemistry degrees from Quaid-i-Azam University Islamabad, Islamabad and Institute of Chemistry, University of the Punjab, Lahore, Pakistan respectively. His research area is synthesis, characterization and applications of metal nanoparticles fabricated in microgels, composites of metal oxides and sulfides and their photocatalytic activity against pollutants, and ligands.*

## 1. Introduction

The exponential increase in industrial activities over the past few decades, especially in textiles, dyeing, pharmaceuticals, leather tanning, paper manufacturing, and cosmetics has led to the indiscriminate release of synthetic dyes into aquatic ecosystems.<sup>1–4</sup> These dyes (often composed of complex aromatic structures<sup>5–8</sup> and xenobiotic constituents<sup>9,10</sup>) pose significant risks to environmental and human health due to their toxicity, carcinogenicity, and resistance to biodegradation.<sup>11–13</sup> Their persistence in water bodies leads to reduced light penetration, oxygen depletion, and disruption of aquatic biodiversity. Therefore, the development of cost-effective, sustainable, and environmentally friendly technologies for the efficient removal or degradation of dye pollutants is a critical global concern.

Various methods have been used for removal of dyes from water, but photocatalysis has garnered substantial attention due to its potential to completely mineralize organic pollutants into less toxic end products such as CO<sub>2</sub> and H<sub>2</sub>O under light irradiation.<sup>14,15</sup> It offers advantages such as simplicity, minimal sludge production, and the potential to harness solar energy. Traditional metal oxide photocatalysts like titanium dioxide (TiO<sub>2</sub>) and zinc oxide (ZnO) have been widely studied and utilized due to their high photocatalytic performance under UV light. However, their wide band gap energy (3.2 eV for TiO<sub>2</sub> and 3.3 eV for ZnO) restricts their activity under visible light, which



constitutes a major portion of the solar spectrum.<sup>16–18</sup> Moreover, certain challenges like electron–hole recombination, limited light absorption, and instability under long-term are present which limit their practical implementation.

Metal sulfide semiconductors like cadmium sulfide (CdS), zinc sulfide (ZnS), copper sulfide (CuS), and molybdenum disulfide (MoS<sub>2</sub>) have emerged as the most suitable alternatives which resolve such issues. These materials possess relatively narrow band gaps, which enable efficient absorption of visible light. For instance, CdS (band gap 2.4 eV) can harness visible light more effectively than TiO<sub>2</sub>, enhancing solar energy utilization in photocatalytic systems. Furthermore, the redox potentials of metal sulfides enable favorable generation of reactive oxygen species (ROS) (hydroxyl radicals ( $\cdot\text{OH}$ ) and superoxide anions ( $\text{O}_2^{\cdot-}$ )) which are responsible for the degradation of dye molecules.<sup>19,20</sup> However, the practical application of metal sulfides is still challenged by photocorrosion, agglomeration in aqueous media, leaching of toxic metal ions (especially in the case of CdS), and rapid recombination of photogenerated charge carriers.<sup>21</sup>

Metal sulfide composite with biodegradable material is the best solution for this issue.<sup>22–26</sup> Metal sulfide–chitosan based composites are the best to resolve these challenges and further enhance the photocatalytic performance and environmental compatibility for metal sulfides in composite form.<sup>27,28</sup> Chitosan (a naturally abundant polysaccharide obtained by deacetylation of chitin (found in crustacean shells)) is recognized for its unique physico-chemical and functional properties. It is biodegradable, non-toxic, biocompatible, and rich in functional groups like amino and hydroxyl moieties that facilitate chelation with metal ions and hydrogen bonding with dye molecules.<sup>29,30</sup> These features make chitosan an excellent support matrix for photocatalytic materials.

Incorporation of metal sulfides into the chitosan matrix offers multiple advantages.<sup>31–34</sup> First, chitosan serves as a stabilizing agent which prevents nanoparticle agglomeration and improves the dispersion of metal sulfide particles, thus increasing the active surface area for photocatalysis.<sup>35–37</sup> Second, the adsorptive nature of chitosan allows for the pre-concentration of dye molecules near the catalytic sites, which enhances degradation efficiency.<sup>15</sup> Third, the polymeric matrix can act as an electron mediator, facilitating the separation of photogenerated electrons and holes and thereby reducing charge recombination. Fourth, chitosan provides mechanical and chemical stability, prolonging the durability and reusability of the composite materials.<sup>38</sup> Additionally, in cases where magnetic components like Fe<sub>3</sub>O<sub>4</sub> are included, the composites can be magnetically recovered, contributing to recyclability and process sustainability.<sup>39</sup>

This review aims to provide a comprehensive analysis of the current progress in the development and application of metal sulfide–chitosan composites for the photocatalytic degradation of dyes. The mechanistic insights of dye degradation pathways, the role of ROS, and the synergistic contributions of chitosan and metal sulfide components are examined.<sup>40</sup> Furthermore, the review delves into the critical factors influencing photocatalytic performance, including band gap energy, surface morphology, surface area, light source, pH,<sup>41–43</sup> and dye concentration<sup>44</sup> *etc.* The environmental impact on the activity of

metal sulfide–chitosan composites has also been discussed with respect to degradation efficiency of dyes.<sup>45,46</sup>

Recent case studies are presented to highlight the photocatalytic capabilities of composites like CdS–chitosan,<sup>47</sup> ZnS–chitosan,<sup>15</sup> and MoS<sub>2</sub>–chitosan<sup>48</sup> in degrading commonly used dyes like methylene blue (MB), rhodamine B (RhB), methyl orange (MO), congo red (CR), acid blue (AB), and crystal violet (CV). Additionally, the review will identify existing research gaps, such as concerns over toxicity (particularly of heavy metal sulfides), long-term stability under irradiation, and performance in real wastewater matrices.

Various review articles are reported on removal of pollutants by metal sulfides<sup>49,50</sup> or organic polymers<sup>51–53</sup> or for specific dye removal,<sup>54–56</sup> but there is no review article on the removal of different dyes by composite based chitosan and metal sulfides. This review specifically focuses on metal sulfide–chitosan composites due to the distinctive synergy between abundant functional groups ( $-\text{NH}_2$  and  $-\text{OH}$ ) of chitosan and the electronic band structures of metal sulfides. Chitosan not only acts as a sustainable support matrix but also enhances photocatalytic performance by improving catalyst dispersion which facilitates interfacial charge transfer, suppress recombination, and promotes dye adsorption through electrostatic and hydrogen-bonding interactions. The mechanistic role of chitosan–metal sulfide interactions (particularly how functional groups of chitosan influence band alignment, surface states, and reactive species generation) remains underexplored and fragmented across the literature. This review fills this knowledge gap by systematically analyzing structure–property relationships, photocatalytic mechanisms, and performance trends of metal sulfide–chitosan composites. Therefore, it provides a unified framework to guide the rational design of next-generation, eco-friendly photocatalysts for dye degradation.

## 2. Photocatalytic degradation mechanism

The mechanism of photocatalytic degradation of dyes by metal sulfide–chitosan based composites relies on the synergistic integration of the semiconductor properties of metal sulfides and the adsorptive, stabilizing, and functionalizing capabilities of chitosan. Basically, the degradation of dyes occurs due to metal sulfides. The bandgap energy values of these metal sulfides are very low, and they obtained these energy values on exposure to suitable light (typically visible light due to the narrow band gap of metal sulfides). They generate the reactive oxygen species (ROS) which effectively breakdown of dye pollutants in several steps as shown in Fig. 1.

In first step, light is adsorbed and electrons–holes are generated. When metal sulfides embedded within the chitosan matrix are irradiated with visible light (or UV light for wider band gap sulfides), they absorb photons whose energy matches or exceeds their band gap energy.<sup>15,57</sup> This excites electrons ( $e^-$ ) from the valence band (VB) to the conduction band (CB) and leave behind positive holes ( $h^+$ ) in the VB as given in eqn (1):



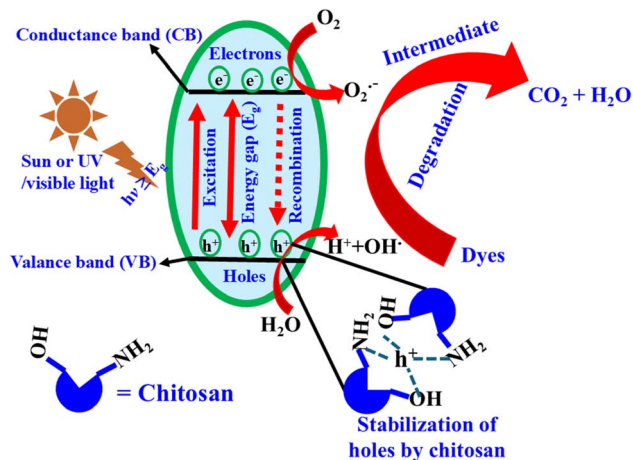
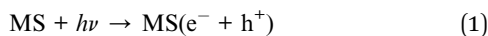


Fig. 1 Photocatalytic degradation mechanism of dyes by metal sulfide–chitosan based composites.



In the second step, the electrons are shifted from VB to CB by absorbing energy. In conventional systems, recombination of the photogenerated electron–hole pairs is a major limitation. However, in the chitosan-supported system, the polymer matrix plays a crucial role in stabilizing and facilitating charge separation. The amine ( $-\text{NH}_2$ ) and hydroxyl ( $-\text{OH}$ ) functional groups in chitosan can trap holes, and the structure of polymer can act as a conduit for electron transport which reduces recombination and extends the lifetime of charge carriers.<sup>58</sup>

In the third step, reactive oxygen species are formed. The photogenerated electrons reduce molecular oxygen ( $\text{O}_2$ ) adsorbed on the surface of the composite to form superoxide radicals ( $\text{O}_2^{\cdot-}$ ) as shown in eqn (2), while holes oxidize water or hydroxide ions ( $\text{OH}^-$ ) to generate hydroxyl radicals ( $\cdot\text{OH}$ ) as given in eqn (6).<sup>38,59,60</sup> The generated peroxide radicals react with water molecules to form hydrogen peroxide radicals which form hydrogen peroxide as given in eqn (3) and (4). The hydrogen peroxide decomposes to hydroxyl radicals as given in eqn (5).

Reaction at CB:



Reaction at VB:



These ROS are highly reactive and play a central role in the oxidative degradation of dye molecules.

In the fourth step, the chitosan component enhances the adsorption of dye molecules through electrostatic interactions, hydrogen bonding, and van der Waals forces. This local

concentration of pollutants near the reactive sites significantly enhances degradation kinetics. The protonated amine groups of chitosan at acidic pH attract anionic dyes, while hydroxyl groups facilitate hydrogen bonding.<sup>61</sup>

In the fifth step, the generated ROS attack the adsorbed dye molecules and break their chromophoric structures and convert them into smaller, less toxic, and often colorless end-products like  $\text{CO}_2$  and  $\text{H}_2\text{O}$ .



Depending on the type of dye (azo, anthraquinone, etc.), different intermediate products may form before complete mineralization.<sup>15</sup> Advanced analysis such as LC-MS or FTIR is often employed to monitor the breakdown pathways.

Heterojunction formation between metal sulfides is a powerful strategy to enhance photocatalytic performance by improving light harvesting which promotes charge separation and regulate ROS generation.<sup>47</sup> When two metal sulfides (supposed X-MS and Y-MS) with different band structures are coupled, an interfacial electric field is established that drives directional charge transfer and suppresses electron–hole recombination which enable complementary redox reactions. The mechanisms of these photocatalytic degradation reactions are type-I, type-II, Z-scheme, and S-scheme heterojunctions.

Mostly heterojunctions follow type-II, Z-scheme, and S-scheme heterojunctions while type-I is very rarely reported in literature. The type-I mechanism of two metal sulfide named X-MS and Y-MS heterojunction is represented in Fig. 2(A). The VB energy level of X-MS is higher than Y-MS, while the CB of X-MS is lower than CB of Y-MS. In this mechanism, the holes of Y-MS will shift to VB of X-MS. Similarly, the CB electrons of Y-MS will shift to the VB of X-MS. Now, the oxygen molecules reduced to  $\text{O}_2^{\cdot-}$  anion radicals from CB of X-MS, while the water molecules or  $\text{OH}^-$  ions are reduced to hydroxyl radicals.<sup>62,63</sup> These ROS degrade rapidly to the dye molecules from medium.

In a type-II heterojunction, the CB of one sulfide lies at a more negative potential, while the VB of the other is more positive. Upon illumination, photogenerated electrons migrate to the lower CB and holes move to the higher VB and spatially separate charge carriers. For example, X-MS/Y-MS is a heterostructure as shown in Fig. 2(B). The VB energy of X-MS is higher than Y-MS, while CB energy of X-MS is also greater than Y-MS. The CB electrons of X-MS shift to the CB of Y-MS, while VB holes of Y-MS shift to the VB of X-MS. Now the reduction of oxygen molecules occurs from the CB electrons of Y-MS, while the oxidation of water molecules/hydroxide proceed from the VB holes of X-MS. Such type of mechanism reduces recombination and extends carrier lifetimes. However, this charge migration can weaken redox ability because the accumulated electrons and holes occupy less energetic band edges.

Z-Scheme heterojunctions have been developed between metal sulfides with suitably aligned band positions as shown in Fig. 2(C) which resolve these limitations. In Z-scheme architectures, electrons in the CB of the less reductive sulfide (Y-MS) recombine with holes in the VB of the less oxidative sulfide (X-MS) which leave highly energetic electrons and holes in the remaining bands. This



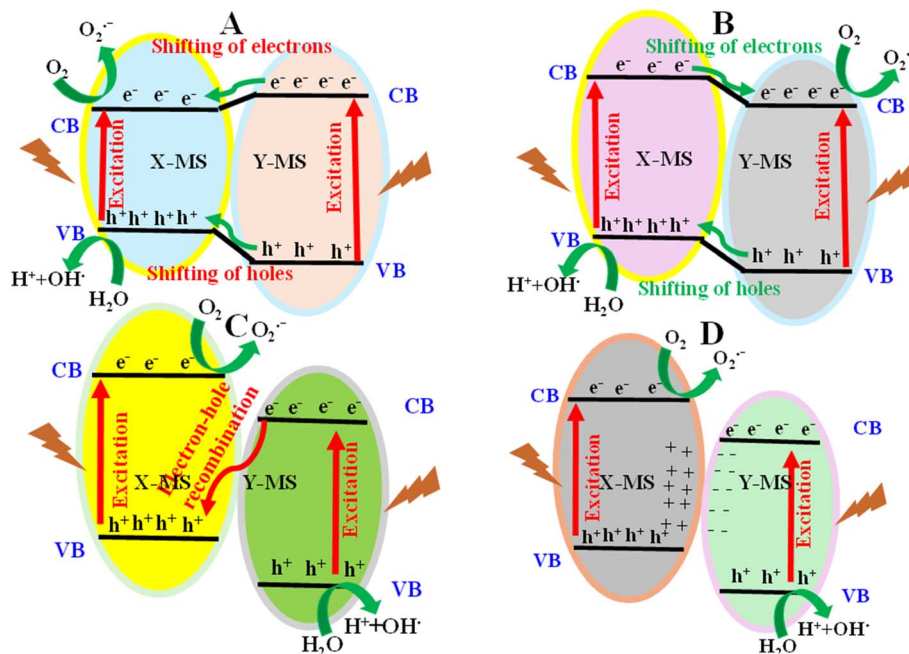


Fig. 2 Photocatalytic degradation mechanisms of two different metal sulfide compounds as (A) type-I, (B) type-II, (C) Z-scheme, and (D) S-scheme heterojunctions.

configuration preserves strong reduction and oxidation potentials which enable simultaneous generation of superoxide ( $O_2^{\cdot-}$ ) and hydroxyl ( $\cdot OH$ ) radicals. Therefore, Z-scheme metal sulfide heterojunctions exhibit superior dye degradation efficiency under visible light.

S-Scheme heterojunctions have been proposed for metal sulfide-metal sulfide systems with intrinsic differences in Fermi levels, such as n-type X-MS coupled with p-type Y-MS as shown in Fig. 2(D). Upon contact, band bending and an internal electric field drive selective recombination of low-energy carriers, while high-energy electrons and holes are retained for redox reactions.<sup>64,65</sup> This mechanism combines the advantages of type-II charge separation with Z-scheme redox preservation which makes S-scheme sulfide heterojunctions particularly effective for visible-light photocatalysis.

In metal sulfide-chitosan composites, the biopolymer matrix further stabilizes heterojunction interfaces by preventing particle agglomeration which facilitates intimate interfacial contact and provides functional groups that act as electron-transfer bridges. Chitosan also enhances adsorption of dye molecules near reactive sites which ensure efficient utilization of the heterojunction-driven ROS pathways. Consequently, heterojunction engineering among metal sulfides (especially when integrated with chitosan) represents a rational design strategy for high-performance, sustainable photocatalysts.

### 3. Photocatalytic activity enhancement of metal sulfide-chitosan based composites by chitosan

The incorporation of chitosan into metal sulfide-based photocatalytic systems significantly enhances their performance in

dye degradation applications, primarily through its multifunctional roles as a stabilizing agent, adsorbent, and facilitator of charge separation. Unique structural and chemical properties of chitosan like biodegradability, high surface area, chelating ability, and protonable amino groups make it an ideal candidate for designing hybrid nanocomposites with superior photocatalytic efficiency.<sup>66,67</sup> The photocatalytic activity of MS-CS composites is enhanced by chitosan as follows.

#### 3.1. Chitosan content effect on photocatalytic activity of metal sulfide-chitosan based composites

The amount of chitosan incorporated into metal sulfide-chitosan composites plays a decisive role in determining their photocatalytic efficiency. Chitosan serves not only as structural support but also as a functional interface that modulates pollutant adsorption, charge separation, nanoparticle morphology, and overall photocatalytic dynamics. When appropriately balanced, chitosan enhances photocatalytic degradation by improving dye adsorption due to its abundant amino and hydroxyl groups, which interact with pollutant molecules through electrostatic forces and hydrogen bonding. This interaction leads to a localized concentration of dyes near the metal sulfide surface and facilitates more efficient attack by photogenerated reactive species such as hydroxyl and superoxide radicals.<sup>15</sup>

Photocatalytic performance is highly dependent on the content of chitosan used. At low chitosan levels, metal sulfide nanoparticles may agglomerate due to insufficient stabilization, resulting in decreased surface area and poor light utilization. Additionally, the limited availability of functional groups reduces dye capture and limits the synergistic benefits of chitosan. In contrast, moderate or optimal chitosan content



provides a porous matrix that enhances dye uptake, improves the dispersion of metal sulfide nanoparticles, and aids in the separation of photogenerated electron-hole pairs. The amine groups in chitosan can trap holes or electrons, temporarily prevent recombination and extend the lifetime of charge carriers for redox reactions. This balanced configuration results in enhanced generation of reactive oxygen species and greater photocatalytic activity. On the other hand, excessive chitosan content can become counterproductive. A thick chitosan coating may insulate the active sites, hindering charge transfer between the dye molecules and the metal sulfide surface. Moreover, it can block incident light and limit the penetration of the necessary photons to excite the semiconductor.<sup>68</sup> The overabundance of chitosan may also reduce the effective surface area of exposed metal sulfide particles and slow the diffusion of reactants through the polymer matrix. In some cases, excessive chitosan leads to mechanical instability or swelling, which disrupts the nanostructure and negatively affects performance.<sup>66</sup> Additionally, the amount of chitosan directly influences the photostability of composite. Metal sulfides (particularly CdS and ZnS) are susceptible to photo-corrosion, which leads to structural degradation and toxic ion release. Adequate chitosan coverage forms a protective shell around the particles, shielding them from oxidative damage and chelating any leached metal ions, thereby prolonging catalyst life and reducing environmental risks. Thus, finding the optimal chitosan content is crucial, not only for maximizing photocatalytic efficiency but also for ensuring reusability, environmental safety, and structural integrity of the composite.

Vijayan and his coworker<sup>69</sup> have synthesized the silver sulfide-chitosan (Ag<sub>2</sub>S-CS) composite with different content of CS (0%, 0.2%, 0.4%, 0.6%, and 0.8%). They reported that the value of the band gap decreases from 0.92 eV to 0.82 eV when the content of CS increased from 0% to 0.8% respectively. This decreasing band gap enhanced the photocatalytic activity of Ag<sub>2</sub>S-CS up to a specific level. After this level of content, electron-hole recombination process dominates which reduces the photocatalytic activity of composites. Therefore, optimized conditions should be identified in this type of study.

The photocatalytic performance of metal sulfide-chitosan composites is highly sensitive to the chitosan content. While low or excessive amounts can hinder performance due to aggregation or shielding effects, an optimized chitosan concentration enhances dye adsorption, improves charge dynamics, and stabilizes the catalyst. Careful tuning of this parameter is essential for designing efficient, recyclable, and sustainable photocatalytic systems for dye degradation and broader environmental remediation. More research is required in this field in future direction.

### 3.2. Improved dye adsorption and pollutant concentration

Chitosan is well known for its ability to adsorb a wide range of pollutants, including anionic and cationic dyes. Its amino (-NH<sub>2</sub>) and hydroxyl (-OH) groups facilitate strong electrostatic and hydrogen bonding interactions with dye molecules. When integrated into metal sulfide photocatalysts, chitosan acts as an

effective dye concentrator, localizing pollutants in close proximity to reactive sites. This pre-concentration not only increases the likelihood of photocatalytic attack by reactive oxygen species (ROS) but also enhances the degradation rate significantly.<sup>70</sup> The high surface area and porosity of chitosan enable it to act as a pollutant trap, particularly under varying pH conditions, where protonated amine (-NH<sub>3</sub><sup>+</sup>) groups attract anionic dyes and hydroxyl functionalities interact with cationic contaminants. This dual functionality makes chitosan exceptionally effective in heterogeneous wastewater systems, leading to enhanced localized concentrations of dyes around the centers of catalyst. Bhat *et al.*<sup>71</sup> have synthesized zinc sulfide-chitosan (ZnS-CS) composite and used them for photocatalytic degradation of acid red-I (AR-I) and crystal violet (CV) dyes. The percentage degradation values of AR-I and CV were found 90.67% and 93.44% in 120 min respectively and the degradation rate of these dyes were 0.021 min<sup>-1</sup> for CV and 0.018 min<sup>-1</sup> for AR-I. Greater photocatalytic activity against CV was due to positive charge in the structure of CV. Therefore, the composite has high interaction with positive charge as compared to negative charged species like AR-I. Therefore, ZnS-CS showed greater photocatalytic performance against CV as compared to AR-I.

The ability of chitosan to form films, beads, or hydrogels provides tunable morphologies that optimize pollutant interaction, swelling behavior, and diffusion dynamics factors that collectively boost the overall photocatalytic degradation kinetics.

### 3.3. Enhanced charge separation and reduced recombination

A critical obstruction in metal sulfide-based photocatalysts like CdS, ZnS, and MoS<sub>2</sub> is the rapid recombination of photogenerated electron-hole pairs, which drastically limits their quantum efficiency. Chitosan integration addresses this by promoting enhanced charge separation and suppressing charge recombination. The nitrogen-containing functional groups (-NH<sub>2</sub>) in chitosan act as electron donors, capturing and temporarily stabilizing photogenerated holes, which delays recombination.<sup>68</sup> This temporary sequestration enhances the availability of free electrons and holes to participate in redox reactions, thereby increasing the generation of ROS such as hydroxyl and superoxide radicals responsible for dye degradation.

The semi-conductive nature of chitosan can facilitate interfacial charge transfer, when interacting with the conduction and valence bands of metal sulfides, enabling a more efficient flow of photogenerated charges between the polymer matrix and the semiconductor. The interpenetrating structure formed by chitosan with dispersed nanoparticles can also create additional heterojunction interfaces, which act as built-in electric fields favoring directional charge migration.<sup>72</sup> The synergy of these interactions improves not only the photocatalytic efficiency but also the photostability and lifecycle of the composite catalyst.<sup>73</sup> This mechanism has particular significance for environmental remediation, where maintaining long-term



photocatalyst efficiency under variable light and aqueous conditions is essential.<sup>38</sup>

Sheshmani and his coworker<sup>43</sup> have synthesized ZnS-CS composite. The band gap value of ZnS reduced from 4.25 eV to 2.60 eV on composition with CS. In this way, the CS facilitates transporting the electron from VB to CB due to decreasing the band gap value. The degradation of brilliant blue FCF (BBFCF) and acid orange-II (AO-II) with ZnS was found 98.77% and 81.87% while this value was 100% and 97.99% with ZnS-CS in the UV irradiation.

### 3.4. Morphological control and surface area enhancement

The morphology and surface characteristics of photocatalytic materials play a pivotal role in dictating their efficiency in degrading dyes. Metal sulfide-chitosan composites benefit significantly from the ability of chitosan to tailor and control these morphological features during synthesis. Chitosan serves as a soft-template and stabilizer, allowing uniform nucleation and controlled growth of metal sulfide nanoparticles like CdS, ZnS, and AgS thereby preventing aggregation and producing nanostructures with high dispersion.<sup>74</sup> This fine dispersion increases the number of accessible active sites for photocatalytic reactions, enhancing dye interaction and degradation.<sup>70</sup>

The inherent porosity and high surface area of chitosan matrices (whether in hydrogel, bead, or membrane forms) promote greater diffusion and adsorption of dye molecules toward the catalyst surface. This not only improves mass transport but also concentrates pollutants in close proximity to reactive sites, which is critical for the generation and transfer of reactive oxygen species. The presence of chitosan also modulates the pore size distribution of composites and surface roughness, creating hierarchical architectures favorable for light trapping and dye capture.<sup>15</sup>

Chitosan enables the design of tailored morphologies like core-shell structures, nanofibers, and hollow spheres, which can significantly influence charge carrier mobility, light harvesting efficiency, and catalytic lifetime. These morphological enhancements translate into improved photocatalytic performance and recyclability of the composite. Thus, by acting as a morphological modulator, chitosan not only optimizes the physical structure but also enhances the catalytic microenvironment for efficient dye degradation.

### 3.5. Stabilization of metal sulfides

One of the major limitations of metal sulfide-based photocatalysts (especially CdS, ZnS, and CuS) is their tendency to undergo photo-corrosion under prolonged light irradiation, particularly in aqueous environments. This degradation occurs when photoinduced holes ( $h^+$ ) oxidize the sulfide anions within the semiconductor lattice itself which leads to structural breakdown and leaching of metal ions into the surrounding medium. Such processes not only diminish the long-term performance of photocatalyst but also pose toxicological risks, especially with heavy metal ions like  $Cd^{2+}$ .<sup>75,76</sup>

Incorporating chitosan into metal sulfide photocatalytic systems offers a multifaceted strategy to mitigate these challenges. As a natural biopolymer rich in amino ( $-NH_2$ ) and hydroxyl ( $-OH$ ) groups, chitosan interacts strongly with metal cations *via* chelation, electrostatic interactions, and hydrogen bonding. When used as a protective matrix or coating, chitosan can physically shield metal sulfide nanoparticles from direct oxidative attack, thereby reducing surface oxidation and stabilizing their chemical structure.<sup>77</sup>

The chelating ability of chitosan plays a crucial role in trapping any released metal ions, preventing their dispersion into the environment. For instance,  $Cd^{2+}$  ions released during photo-corrosion can be sequestered by the chitosan matrix, minimizing secondary pollution. This ion-capturing mechanism is particularly relevant for environmental remediation applications, where safety and ecological compatibility are vital. In addition, chitosan can form core-shell or matrix-dispersed structures with metal sulfides that enhance structural integrity and slow the degradation process. It also contributes to charging carrier stabilization by passivating surface defects that would otherwise accelerate photo-corrosion.<sup>68</sup>

These attributes of chitosan not only extend the lifespan of metal sulfide photocatalysts under operational conditions but also enhance their environmental safety profile. This makes chitosan a critical additive for developing stable, recyclable, and green photocatalytic systems for dye degradation and wastewater treatment.

### 3.6. Functionalization and hybrid engineering

The versatility of chitosan as a polymeric matrix enables extensive functionalization and hybrid engineering, which significantly enhances the photocatalytic performance of metal sulfide-chitosan-based composites. This strategy involves chemical modification of chitosan or the integration of co-catalysts, nanomaterials, or dopants into the composite to tune its structural, optical, and electronic properties.

Chitosan possesses reactive amino ( $-NH_2$ ) and hydroxyl ( $-OH$ ) groups, which can be chemically modified or grafted with functional moieties like carboxyl, sulfonic, or phosphonic acids. These modifications improve solubility, adsorption capacity, and interaction with dye molecules or metal sulfide nanoparticles. For example, carboxymethyl chitosan can enhance water dispersibility and metal ion coordination, leading to more stable and active photocatalytic composites.

Hybrid engineering further allows the incorporation of co-functional materials, such as:

(1) Graphene oxide (GO) or reduced graphene oxide (rGO), which enhances electron mobility and prevents charge recombination.<sup>35</sup>

(2) Noble metal nanoparticles (*e.g.*, Ag, Au, Pt), which act as electron sinks and plasmonic enhancers to improve light absorption.<sup>78</sup>

(3) Magnetic nanoparticles (*e.g.*,  $Fe_3O_4$ ), which impart magnetic recoverability to the photocatalyst, enabling efficient recycling.<sup>39</sup>



(4) Carbon dots or quantum dots, which expand light absorption into the visible range and facilitate multi-electron transfer processes.

Chitosan can serve as a structural scaffold to form core-shell, layered, or heterojunction architectures with metal sulfides. Such hybrid configurations improve interfacial contact, charge carrier dynamics, and light harvesting by creating synergistic interactions between components. For example, Sheshmani and his coworker<sup>45</sup> have synthesized CdS-rGO and CdS-CS-rGO composites and used them for degradation of acid orange-VII (AO-VII). The degradation efficiency of AO-VII with CdS-rGO was found lower than CdS-CS-rGO due to less electron mobility and high charge recombination in CdS-rGO. The degradation efficiency of CdS-rGO was found 14.92% while that of CdS-CS-rGO was 89.26%. For instance, CdS-chitosan-GO ternary composites show higher photocatalytic activity than binary systems due to improved charge separation and broader light absorption. Similarly, ZnS-chitosan-Ag hybrids exhibit enhanced photocatalytic dye degradation under visible light through surface plasmon resonance effects of silver.

Functionalization and hybrid engineering of chitosan in metal sulfide-based systems unlock new dimensions in composite design. These tailored nanostructures offer improved photocatalytic efficiency, structural integrity, and adaptability to various environmental conditions, making them powerful candidates for sustainable pollutant degradation technologies.

### 3.7. Green chemistry and recyclability

The integration of chitosan into metal sulfide-based photocatalytic systems strongly aligns with the principles of green chemistry and enhances the recyclability of the resulting composites. Chitosan is inherently renewable, biodegradable, non-toxic, and readily available which makes it an ideal candidate for sustainable material design in environmental remediation. One of the most critical aspects of green photocatalysis is reducing the ecological footprint of both the materials used and the processes employed. Traditional synthetic polymers or chemical binders often involve toxic reagents and are non-degradable. In contrast, chitosan-based composites can be fabricated using mild, aqueous-phase processes, often at ambient temperatures, with minimal use of hazardous solvents or additives. This green synthesis route significantly reduces energy consumption and chemical waste generation.

Chitosan also enables the creation of recyclable and reusable photocatalysts. Its film-forming and gelation properties allow the metal sulfide nanoparticles to be embedded into stable matrices, which prevents leaching and loss of the active photocatalyst during treatment cycles.<sup>38</sup> For example, Bhat *et al.*<sup>71</sup> have synthesized ZnS-CS. They used this system for degradation of CV and AR-I dyes and reported that ZnS-CS have maintained its photocatalytic activity during recycling as shown in Fig. 3. The stability of ZnS-CS in recycling is due to the presence of CS. If such metal sulfide systems are further combined with magnetic nanoparticles (*e.g.*, Fe<sub>3</sub>O<sub>4</sub>), chitosan-

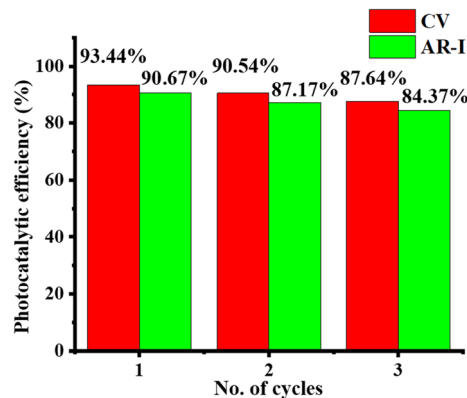


Fig. 3 Photocatalytic performance of ZnS-CS after recycling.<sup>71</sup> Adapted from ref. 71 with permission from American Chemical Society,<sup>71</sup> copyright 2024.

metal sulfide composites can be magnetically separated from treated water, enabling easy recovery and reuse without the need for filtration or centrifugation.

These materials maintain high photocatalytic efficiency over multiple cycles. The structural integrity of chitosan prevents aggregation of the nanoparticles and protects the photocatalyst against degradation (*e.g.*, photo-corrosion) and hence prolongs its operational lifespan. Additionally, post-use disposal of these composites poses minimal risk to the environment due to the biodegradable nature of chitosan and the stabilization of potentially toxic metal ions within the polymeric network. Thus, the use of chitosan not only enhances the photocatalytic degradation of dyes but also facilitates the development of eco-friendly, reusable, and cost-effective treatment platforms, essential for practical deployment in wastewater purification and sustainable environmental technologies.

The recycling of composite has been done by ultra-fast centrifugation machine. During this recycling, leaching of metal sulfide can occur which reduces the photocatalytic performance of chitosan-metal sulfide composite. This leach produces toxicity in the environment. To resolve this, magnetic based composites should be synthesized. Such systems can easily reduce the leaching effect of metal sulfide during recycling under magnetic field.

Excessive content of chitosan in chitosan-metal sulfide composite has some challenges. If the content of chitosan is much greater than metal sulfide, the chitosan itself absorbs UV light and decreases the performance of metal sulfides for photocatalytic degradation. Another disadvantage of excessive chitosan in composite is the system shows adsorption behavior more dominantly than photocatalytic performance. Therefore, it is crucial to maintain the ratio of composite during synthesis. More study is required in this field in near future.

A summary of the influence of chitosan on the photocatalytic activity of metal sulfide-chitosan based composites is described in Table 1.



Table 1 Photocatalytic performance enhancement of metal chitosan on photocatalytic activity of metal sulfide–chitosan based composites

Enhancement factor	Role of chitosan	Effect on photocatalysis	References
Improved dye adsorption	Amino and hydroxyl groups provide binding sites for dyes	Localized dye concentration near reactive sites increases degradation rate	79
Charge separation and recombination suppression	Electron-donating $-NH_2$ and $-OH$ groups stabilize photogenerated holes	Enhanced lifetime of charge carriers increases ROS formation	80
Nanoparticle morphology and dispersion	Acts as a soft template, prevents aggregation	Increased surface area and better exposure to light	81
Photo-corrosion suppression	ZnS–CMCS forms a protective shell around $AgInS_2$	Improves photostability and longevity; reduces metal ion leaching	82
Band gap tuning and light absorption	Slight band alignment/modulation when interacting with metal sulfides	Enhanced absorption in visible region, better solar utilization	83
Functionalization and hybrid structure engineering	Functional groups enable integration with GO	Multifunctionality: magnetism, light absorption, recyclability	84
Recyclability and green chemistry	Biodegradable, non-toxic matrix supports repeated use	Eco-friendly and sustainable alternative to synthetic stabilizers	85
Different environmental conditions (pH, temp, light, magnetic)	Responsive behavior alters adsorption, swelling, and catalyst performance under different environmental cues	Enables tunable activity, intelligent pollutant targeting, and efficiency modulation	86

## 4. Metal sulfide based enhancing factors of photocatalytic activity of metal sulfide–chitosan composites

The photocatalytic activity of metal sulfide–chitosan composites also depends on the behavior of metal sulfides. In this case, the factors which enhance the photocatalytic efficiency of composite material are discussed below.

### 4.1. Nature of metal sulfide

The photocatalytic performance of metal sulfide–chitosan based composites is fundamentally influenced by the nature and intrinsic characteristics of the metal sulfide component as given in Table 2. Metal sulfides are classified as narrow to moderate band gap semiconductors, making them excellent candidates for visible-light-driven photocatalysis which is a key advantage over traditional metal oxides. Among the widely investigated sulfides, cadmium sulfide (CdS) stands out due to its suitable band gap (2.4 eV) and favorable conduction band position for efficient electron transfer during photocatalysis. However, CdS suffers from photocorrosion under illumination, especially in aqueous environments, which limits its long-term stability. When integrated with chitosan, this issue is mitigated due to the formation of protective polymeric layers and enhanced charge transfer pathways.<sup>45</sup> Similarly, zinc sulfide (ZnS), although possessing a wider band gap (3.6 eV), exhibits high quantum efficiency under UV light. When composited with chitosan, the resulting hybrid system demonstrates improved surface area, enhanced dispersion, and better light harvesting through structural modulation and doping strategies, which allow partial activation under visible light.<sup>43</sup> Copper sulfide (CuS) and molybdenum disulfide ( $MoS_2$ ) are increasingly

favoured for visible-light photocatalysis due to their strong light absorption in the visible range and layered structures that support high surface reactivity. CuS offers localized surface plasmon resonance (LSPR) effects, while  $MoS_2$  provides excellent catalytic edge sites. Chitosan incorporation assists in stabilizing these nanosheets, preventing restacking and enhancing their interaction with target dye molecules.<sup>87,88</sup>

The selection of the metal sulfide is critical not only for defining the optical and electronic properties of the composite but also for determining its stability, light utilization, and reactivity. The integration of chitosan allows tailoring of these properties which offer a flexible and green approach to developing next-generation photocatalysts with enhanced performance for environmental remediation.

### 4.2. Compositions of metal sulfides

The composition of metal sulfides (whether monometallic, bimetallic, or doped) plays a critical role in tailoring their electronic structure, optical properties, and redox behavior, ultimately influencing photocatalytic performance. Pure metal sulfides like CdS, ZnS, and CuS exhibit distinct band structures, but often suffer from drawbacks such as photocorrosion (CdS), limited visible light response (ZnS), or insufficient stability (CuS). These limitations have prompted the development of bimetallic sulfides (*e.g.*, ZnFeS, CuZnS, NiCoS) and multi-metal chalcogenides, which combine the advantages of individual components and introduce synergistic effects that enhance light harvesting, charge carrier mobility, and active site distribution.

For instance, Pure CdS and  $C_3N_4$  doped CdS nanoparticles supported on chitosan demonstrated enhanced charge separation due to the internal electric field generated by the metal



Table 2 Summary of comparison of metal sulfide-based composites on the basis of photocatalytic degradation of dyes

Composites	Enhancement factor	Dye degraded	Time (min) and light	Degradation efficiency (%)	References
CdS-CS-rGO	Suppressed photocorrosion, improved charge separation <i>via</i> chitosan	OR-7	60, visible light	89	45
ZnS, ZnS-CS, CdS-ZnS-CS	Band gap tuning <i>via</i> doping and chitosan stabilization	RhB	120, UV light	99	89
CuS-CS-P(VA)	Efficient charge transfer and surface adsorption	MG	60, UV light	96	87
MoS <sub>2</sub> -CS-Fe <sub>3</sub> O <sub>4</sub>	Exfoliation and heterojunction formation	MO	80, simulated solar light	89	39

heterojunction interface, leading to improved dye degradation under visible light.<sup>89</sup> Similarly, CuZnS-chitosan composites benefited from Cu-induced band gap narrowing and Zn-induced stability, achieving superior photocatalytic performance compared to single-metal sulfide analogs. In addition to bimetallic combinations, doped metal sulfides (*e.g.*, Mn-doped CdS or Ag-doped ZnS) have shown great promise. Doping introduces new energy levels within the band structure that facilitate visible light absorption and improved carrier dynamics. Chitosan serves not only as a structural matrix but also plays an active role in modulating dopant distribution through its chelating and coordinating functional groups (*e.g.*, -NH<sub>2</sub> and -OH). This uniform incorporation avoids dopant clustering, which can lead to electron-hole recombination. Moreover, chitosan-stabilized ternary sulfides like NiFe<sub>2</sub>S<sub>4</sub> and CoNi<sub>2</sub>S<sub>4</sub> exhibit superior conductivity, increased electroactive surface area, and redox flexibility, all of which contribute to rapid photocatalytic reaction kinetics.<sup>90</sup> These complex sulfide systems are typically synthesized *via* hydrothermal or solvothermal routes in the presence of chitosan, which acts as a templating and structure-directing agent.

The composition of metal sulfides from mono to bimetallic and doped systems can drastically influence the photocatalytic behavior of chitosan-based composites. The synergistic effects arising from multi-metal interactions, when stabilized and dispersed by chitosan, lead to enhanced visible light absorption, reduced charge recombination, and improved photocatalytic stability.

#### 4.3. Surface area

Surface area directly influences the number of active sites available for photocatalytic reactions. A higher surface area leads to enhanced adsorption of dye molecules and improved interaction between the photocatalyst and pollutants. Metal sulfide-chitosan composites typically benefit from the porous, interconnected network provided by chitosan, which increases the overall surface area of the material. This porous matrix not only facilitates the dispersion of metal sulfide nanoparticles but also allows for rapid diffusion of reactants and light penetration.<sup>35</sup> For example, CdS embedded in a chitosan scaffold exhibited a marked increase in BET surface area and photocatalytic degradation efficiency compared to bare CdS.<sup>45</sup> Additionally, mesoporous structures achieved through chitosan

templating can provide hierarchical porosity, further aiding in pollutant access and degradation kinetics. The addition of another porous material along with chitosan in metal sulfide further enhances the photocatalytic degradation of dyes. The porous material increases the surface area which facilitates the approach of dye molecules on the surface of metal sulfide. Therefore, the degradation efficiency of dyes rapidly increases on the addition of porous material.

#### 4.4. Band gap engineering

Band gap engineering is a crucial strategy to enhance the photocatalytic performance of metal sulfide-chitosan composites by tailoring the electronic structure to improve light harvesting. Narrowing the band gap enables utilization of a broader portion of the solar spectrum, particularly the visible region. In this context, combining metal sulfides with chitosan aids in band gap modulation through various approaches such as heteroatom doping, metal ion incorporation, and hybrid interface design. Chitosan (containing functional groups like -OH and -NH<sub>2</sub>) can chemically interact with metal ions during synthesis to induce defect states or shift the conduction and valence band edges. For example, AC-CuS-chitosan composites have shown reduction in band gap value as compared to pure CuS, attributed to electron delocalization and interfacial interactions between CuS and chitosan.<sup>66</sup> ZnS-chitosan systems have demonstrated improved photocatalytic efficiency through engineered band gap narrowing facilitated by nitrogen atoms in chitosan. These modifications reduce the energy threshold for electron excitation, thus enabling more efficient generation of electron-hole pairs under visible light.<sup>91</sup> Consequently, band gap engineering *via* chitosan incorporation represents a promising avenue for designing light-responsive, efficient photocatalytic materials for wastewater remediation.<sup>62</sup> This band gap can also be further reduced by using porous material in addition to metal sulfide-chitosan composites. These porous materials can facilitate the delocalization of electrons as well as enhance the stability of metal sulfides and hence reduce the band gap. In this way, they enhance the photocatalytic performance of composites. For example, Chola *et al.*<sup>44</sup> have synthesized silica-chitosan-molybdenum (SC-CS-MoS<sub>2</sub>) and applied it for degradation of MB and malachite green (MG). The presence of SC reduces the band gap value and hence increased the dye removal percentage from water. Janani *et al.*<sup>62</sup> have



**Table 3** Effect of composite formation of chitosan with two semi-conductors heterojunction<sup>62</sup>

Photocatalyst	Energy band gap (eV)	Apparent rate constant (min <sup>-1</sup> )
CuO	1.7	0.002
ZnS	3.65	0.001
CuO–ZnO–PVA–CS	2.0	0.007

synthesized a heterojunction of CuO loaded ZnS entrapped poly(vinyl alcohol–chitosan) matrix CuO–ZnS–PVA–CS. They used these semiconductors for photocatalytic degradation of TC. The bandgap value of ZnS (3.65 eV) is higher than CuO (1.7 eV). Therefore, electrons are easily jumping from VB to CB in CuO as compared to ZnS. So, the photocatalytic performance of CuO was found to be greater than ZnS, while the photocatalytic activity of Cu–ZnS–PVA–CS was found more greater than CuO even higher bandgap value (2.0 eV). In this case, the polymers (both PVA and CS) facilitate approaching the pollutant rapidly to the semiconductor surface and degraded more rapidly as given in Table 3. Additionally, this junction formation reduces the electron–hole recombination as compared to CuO and hence shows better photocatalytic activity.

#### 4.5. Non-metal doping

Non-metal doping introduces new electronic states within the band structure of metal sulfides, improving their visible-light photocatalytic efficiency. Elements such as nitrogen (N), sulfur (S), phosphorus (P), and boron (B) are particularly effective in modifying the electronic configuration of metal sulfides to narrow the band gap and enhance light absorption.<sup>92</sup> Chitosan (rich in nitrogen-containing functional groups (*e.g.*, –NH<sub>2</sub>)) acts as a natural nitrogen source during the synthesis process. This facilitates *in situ* doping of nitrogen into the metal sulfide lattice, creating localized energy states within the band gap that enables lower-energy photon absorption as shown in Fig. 4. For example, N-doped C–MnFe<sub>2</sub>O<sub>4</sub>–CuS–CS–O<sub>3</sub> composites have demonstrated superior degradation of methylene blue (MB) under visible light due to the enhanced electron–hole generation and mobility. It degraded 98.14% of MB in just 12 min while degraded more than 90% of MO, RhB, and TC in same duration.<sup>93</sup> Additionally, the incorporation of non-metals improves surface reactivity and adsorption capabilities by modifying surface polarity and hydrophilicity, both critical for efficient dye adsorption. Through this self-doping pathway, chitosan provides a sustainable and effective route for non-metal doping without the need for external dopant sources, aligning with green synthesis principles while achieving enhanced photocatalytic activity.<sup>94</sup>

#### 4.6. Metal doping

Metal doping is an effective method for modifying the photocatalytic behavior of metal sulfides by introducing foreign metal ions into the crystal lattice. This process alters the electronic band structure, facilitates charge carrier mobility, and creates

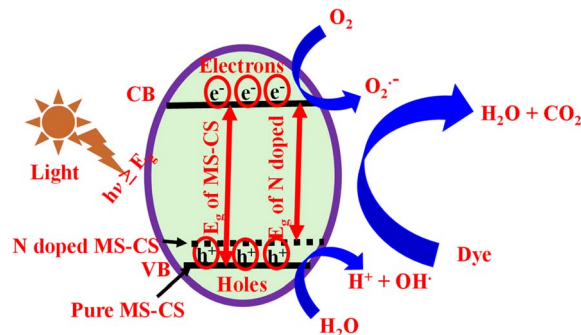


**Fig. 4** Nitrogen doping in metal sulfide–chitosan composite decreases the band gap.

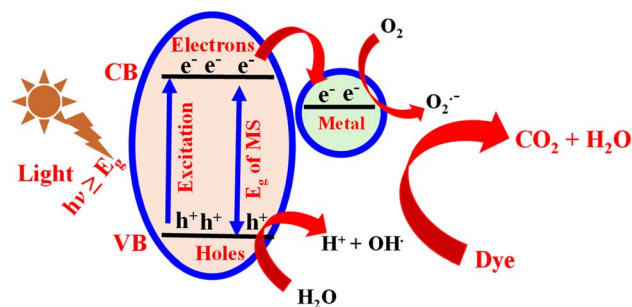


**Fig. 5** Effect of metal doping in the band gap of metal doped metal sulfide–chitosan composites.

defect sites that serve as active centers for photocatalysis as shown in Fig. 5. Transition metals like Ni, Mn, Co, and Fe have been successfully used to dope metal sulfides like CdS and ZnS, resulting in increased light absorption and reduced recombination rates of photogenerated electron–hole pairs. The presence of these dopant ions introduces intermediate energy levels within the band gap, which acts as trap sites to promote charge separation. Chitosan plays a vital role in stabilizing the dopant ions during the synthesis, ensuring homogeneous distribution and preventing agglomeration.<sup>38</sup> For example, Cu- and Fe-doped MoS<sub>2</sub>–chitosan composites have shown superior photocatalytic degradation of rhodamine B (RhB) due to the synergistic effect of metal doping and chitosan-induced dispersion.<sup>95</sup> Additionally, the presence of chitosan enhances the coordination environment of the dopant ions through its functional groups, thereby improving their incorporation efficiency and catalytic activity. Overall, metal doping in the presence of chitosan leads to robust composite systems with improved photocatalytic properties under visible light irradiation.

#### 4.7. Heterojunction engineering

Heterojunction engineering is a powerful strategy for enhancing the photocatalytic performance of metal sulfide–chitosan composites by constructing interfaces between two or more semiconductors with different band structures.<sup>70</sup> These heterojunctions promote efficient charge separation by creating internal electric fields that drive photogenerated electrons and



holes in opposite directions, reducing their recombination probability as shown in Fig. 6. In metal sulfide–chitosan composites, heterojunctions can be formed between metal sulfides (*e.g.*, CdS, ZnS, CuS) and other metal oxides (*e.g.*, TiO<sub>2</sub>, ZnO)<sup>78</sup> or even between different sulfides (*e.g.*, CdS–MoS<sub>2</sub>).<sup>38</sup> Chitosan serves as a structural and chemical bridge that enhances the interfacial contact between the components, facilitating the formation of intimate junctions.<sup>62</sup> Moreover, chitosan can stabilize these structures and prevent nanoparticle aggregation. For instance, a CoS<sub>2</sub>–CeO<sub>2</sub> heterojunction anchored on a chitosan scaffold exhibited significantly higher photocatalytic degradation efficiency due to synergistic charge transfer dynamics and improved pollutant adsorption.<sup>96</sup> Z-Scheme and type-II heterojunction architectures are particularly beneficial in preserving high redox potential while ensuring spatial charge separation. Through precise heterojunction engineering enabled by chitosan, the response of photocatalyst to visible light and redox efficiency can be simultaneously optimized. Kiani *et al.*<sup>78</sup> have synthesized Ag<sub>3</sub>PO<sub>4</sub>, CdS, Ag<sub>3</sub>PO<sub>4</sub>–CdS, Ag<sub>3</sub>PO<sub>4</sub>–CdS–CS, and Pt–Ag<sub>3</sub>PO<sub>4</sub>–CdS–CS and used them for photocatalytic degradation of MB under aqueous medium in visible light irradiation. The degradation efficiency of Ag<sub>3</sub>PO<sub>4</sub>–CdS was greater than pure Ag<sub>3</sub>PO<sub>4</sub> and CdS due to decreasing band gap value. The photocatalytic degradation further enhanced by using chitosan along with Ag<sub>3</sub>PO<sub>4</sub>–CdS to form Ag<sub>3</sub>PO<sub>4</sub>–CdS–CS. The CS increases the surface area and approach of MB to the surface of Ag<sub>3</sub>PO<sub>4</sub>–CdS. The degradation efficiency of Ag<sub>3</sub>PO<sub>4</sub>–CdS was 53% while that of Ag<sub>3</sub>PO<sub>4</sub>–CdS–CS was 81%. This degradation is further increased on doping of metal in Ag<sub>3</sub>PO<sub>4</sub>–CdS–CS.

#### 4.8. Plasmonic enhancement

Plasmonic enhancement leverages the localized surface plasmon resonance (LSPR) effect of noble metal nanoparticles like silver (Ag) and gold (Au) to boost the photocatalytic activity of metal sulfide–chitosan composites. When excited by visible light, these plasmonic nanoparticles generate strong electromagnetic fields near their surface, promoting efficient light harvesting and hot electron injection into the conduction band of the adjacent semiconductor. This process significantly

enhances charge separation and expands light absorption into the visible or even near-infrared region. Chitosan serves as a biopolymeric stabilizer that anchors plasmonic nanoparticles onto the metal sulfide surface, preventing aggregation and facilitating strong interfacial contact. For instance, Ag-decorated ZnS–chitosan composites demonstrated higher photocatalytic degradation of organic dyes under visible light due to enhanced light absorption and interfacial charge transfer.<sup>25</sup> Moreover, the functional groups of chitosan can interact with both the metal sulfide and plasmonic particles, forming a conductive bridge that aids in electron transfer. Thus, the integration of plasmonic nanoparticles within chitosan-stabilized sulfide composites offers a synergistic route to develop highly efficient photocatalysts for environmental remediation.<sup>97</sup>

#### 4.9. Nature and intensity of light

Light intensity and nature of light play a crucial role in dictating the rate and extent of photocatalytic reactions in metal sulfide–chitosan based systems.<sup>77</sup> The generation of electron–hole pairs in semiconductors like CdS or ZnS is directly dependent on the photon flux received by the material. Higher light intensity generally leads to an increase in the number of photogenerated charge carriers, thereby enhancing the photocatalytic activity. However, beyond a certain threshold, the rate of electron–hole recombination may also rise, potentially limiting the photocatalytic efficiency. Chitosan-modified composites can help mitigate such losses by improving charge carrier separation and facilitating rapid electron transfer.<sup>98</sup> For instance, under intensified visible-light irradiation, metal sulfide–chitosan composites showed improved degradation kinetics of dyes compared to pure metal sulfide, attributed to chitosan-mediated suppression of recombination. Moreover, the film-forming nature of chitosan can create thin layers that ensure uniform light absorption and reduce photonic scattering losses. Thus, optimizing light intensity and tuning chitosan content are vital strategies for maximizing photocatalytic performance under different illumination conditions.

Sheshmani and his coworker<sup>43</sup> has synthesized ZnS–CS and used it for photocatalytic degradation of acid orange-II (AO-II) and brilliant blue FCF (BBFCF). They studied the degradation efficiency of both ZnS and ZnS–CS in dark, UV irradiation and visible irradiation. They obtained that the photocatalytic degradation efficiency of ZnS–CS was greater than ZnS and the degradation efficiency in visible irradiation was greater than UV irradiation condition. ZnS degraded to 98.77% and 81.87% of BBFCF and AO-II dyes in UV irradiation while this degradation efficiency was 95.23% and 70.64% in visible irradiation respectively. Similarly, the degradation efficiency of BBFCF and AO-II with ZnS–CS was found 100% and 97.99% respectively in UV irradiation while 100% and 80.00% in visible irradiation.

#### 4.10. Scavengers

Scavengers are chemical agents that are deliberately added to photocatalytic systems to selectively quench specific reactive species, allowing researchers to identify the dominant reactive

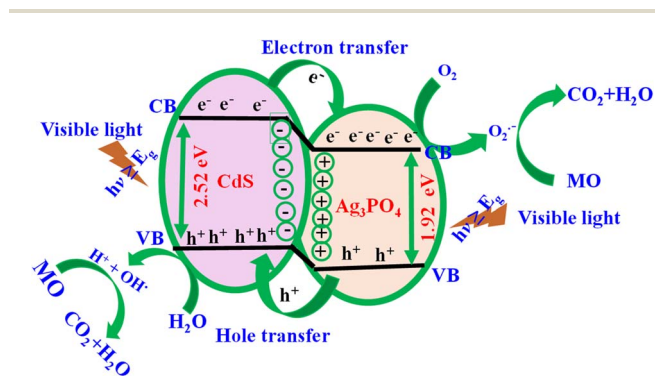


Fig. 6 Junction formation during using Ag<sub>3</sub>PO<sub>4</sub> and CdS along with CS to degrade dye.<sup>78</sup> Adapted from ref. 78 with permission from MDPI,<sup>78</sup> copyright 2020.



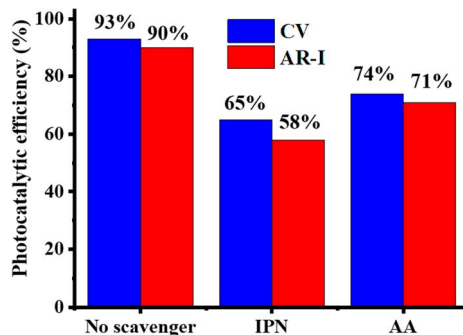


Fig. 7 Effect of scavengers on photocatalytic activity of ZnS-CS against acid red-I (AR-I) and crystal violet (CV).<sup>71</sup> Adapted from ref. 71 with permission from American Chemical Society,<sup>71</sup> copyright 2024.

oxygen species (ROS) responsible for photocatalytic degradation. In the context of metal sulfide-chitosan based composites, scavengers help elucidate the mechanisms behind dye degradation by targeting photogenerated electrons, holes, hydroxyl radicals ( $\cdot\text{OH}$ ), or superoxide radicals ( $\text{O}_2^{\cdot-}$ ). For instance, isopropanol (IPN) is commonly used as a hydroxyl radical scavenger, while benzoquinone (BQ) targets superoxide radicals.<sup>99</sup> The addition of scavengers during photocatalysis experiments often results in decreased degradation efficiency, indicating the key role of the targeted ROS. Chitosan may also influence ROS generation and distribution due to its surface functional groups and electron-donating nature. Furthermore, scavengers aid in optimizing catalyst design by highlighting limitations in charge carrier utilization or ROS production. For example, a SnS-chitosan composite tested with various scavengers revealed that both  $\cdot\text{OH}$  and  $\text{O}_2^{\cdot-}$  were central to the degradation of CV, with the suppression of activity in the presence of IPN and BQ confirming their involvement.<sup>85</sup> Bhat *et al.*<sup>71</sup> have also studied the photocatalytic activity of ZnS-CS against CV and AR-I. They used

IPN and ascorbic acid (AA) as scavengers. The photocatalytic activity of ZnS-CS was found greater in the absence of these scavengers as shown in Fig. 7. Hence, the systematic use of scavengers provides valuable insight into photocatalytic pathways and enhances the rational design of efficient metal sulfide-chitosan photocatalysts.

Photocatalytic activity of metal sulfide-chitosan composites is governed by a complex interplay of material composition, structural features, and reaction parameters. Understanding and optimizing these variables enables the development of highly efficient, stable, and eco-friendly catalysts for dye degradation in wastewater treatment.

Different parameters which are controlled with metal sulfide in metal sulfide-chitosan composites are summary in Table 4.

## 5. Environmental impact on photocatalytic performance of metal sulfide-chitosan based composites

The integration of chitosan into metal sulfide-based composites improves their photocatalytic efficiency under different degradation environment.<sup>101</sup>

### 5.1. pH

The pH of medium directly impact on the photocatalytic performance of metal sulfide-chitosan based composites particularly in dye degradation applications. This performance is due to the chemical nature of chitosan, which contains abundant amino ( $-\text{NH}_2$ ) and hydroxyl ( $-\text{OH}$ ) groups in their structure that can undergo protonation and deprotonation in response to the surrounding pH. This pH sensitivity translates into changes in surface charge, dye affinity, and ultimately, photocatalytic performance.

Table 4 Summary of photocatalytic activity enhancement of metal sulfide-chitosan composites

Factors	Enhancement	Effect	Dye	Time (min)	Degradation efficiency (%)	References
Composition of metal sulfide	Tailors synergistic effects and redox behavior	ZnFeS shows superior dye degradation than pure ZnS	MB, MO	90	91–96	89
Surface area	Increases number of reactive sites	MXene-ZnS-chitosan-cellulose matrices enhance adsorption and kinetics	MB, EBT, and AB-80	—	100	86
Band gap engineering	Expands light absorption to visible region	CS-GO-MoS <sub>2</sub> shows red-shifted absorption edge	MO	—	99	100
Non-metal doping	Introduces intermediate energy levels	N-Doping <i>via</i> chitosan enhances visible light absorption	MB, and MO, RhB, CT	12	98 and >90	93
Heterojunction engineering	Promotes directional charge transfer	Cu <sub>2</sub> MoS <sub>4</sub> decorated WO <sub>3</sub> embedded in chitosan shows synergistic photocatalysis	CV	80	100	42
Plasmonic enhancement	Boosts visible-light absorption and hot electron transfer	Ag-CdS-chitosan composite exhibits LSPR-assisted activity	MB	20	96	25
Scavengers	Clarify active species and optimize performance	IPN and BQ reveal $\cdot\text{OH}$ and $\text{O}_2^{\cdot-}$ are key ROS in ZnS-CS	CV and AR-I	120	93 and 90 respectively	71



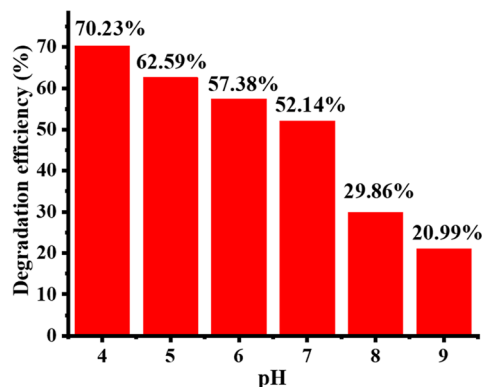


Fig. 8 pH of medium controlled the photocatalytic efficiency of CdS-CS-rGO composite against AO-VII dye.<sup>45</sup> Adapted from ref. 45 with permission from Springer Nature,<sup>45</sup> copyright 2024.

Under acidic conditions, the amino groups on chitosan become protonated to form  $\text{-NH}_3^+$  groups which impart a positive charge to the composite surface. This electrostatic environment enhances the adsorption of negatively charged (anionic) dyes like methyl orange (MO), Congo red (CR), or acid blue (AB), concentrating them near the active sites of the metal sulfide photocatalyst. As a result, the pre-concentration of pollutants at the interface boosts the efficiency of photogenerated ROS in breaking down dye molecules. Conversely, in alkaline media, deprotonation of the amino groups leads to a reduction in positive surface charge which decreases electrostatic attraction for anionic dyes but potentially increases interaction with cationic pollutants. Furthermore, changes in surface charge at different pH values also influence the zeta potential, stability, and dispersion of the nanocomposite in solution, affecting light penetration and catalyst-pollutant contact efficiency.<sup>75</sup> Additionally, the pH of the medium also affects the formation of  $\text{O}_2^-$  through photocatalytic reactions as given in equations from 2 to 5. In this way, the photocatalytic performance is higher in acidic condition than neutral conditions.<sup>77</sup>

Sheshmani and his coworker<sup>45</sup> studied the effect of pH on photocatalytic degradation of CdS-rGO and CdS-CS-rGO composites against acid orange-VII (AO-VII) dye. The pH effect on the photocatalytic efficiency of CdS-rGO is smaller than CdS-CS-rGO. The degradation efficiency of CdS-rGO decreased from 13.08% to 8.63% on increasing the pH from 4 to 9 respectively as shown in Fig. 8. This decline in photocatalytic activity is due to production of similar charge on both CdS-rGO and AO-VII on increasing the pH of medium. Therefore, repulsion takes place which reduced the adsorption of dyes on the surface of composite. This decreasing efficiency was greater in the case of CdS-CS-rGO composite. In this composite, positive charge is present in the network of CdS-CS-rGO due to protonation of amino groups of CS at low pH. At low pH, the amino ( $\text{-NH}_2$ ) groups of composites are shifted into protonated ( $\text{-NH}_3^+$ ) form. These positive parts of composites strongly interact with negative structured AO-VII dye which results in high degradation. Therefore, maximum interactions are present

between them. So, maximum degradation occurred at low pH (70.23% at pH 4). These protonated ( $\text{-NH}_3^+$ ) forms are shifted into deprotonated ( $\text{-NH}_2$ ) forms. Therefore, the electrostatic attraction reduces which decreases the photocatalytic degradation efficiency of composite. Therefore, degradation efficiency decreased at high pH (20.99% at pH 9).

If a copolymer is used during synthesis of composite which contain carboxylic group in their structure. In this case, the composites have both acidic ( $\text{-COOH}$ ) and basic ( $\text{-NH}_2$ ) groups in their structure. In this case, the composites are in a swelling state at both strong acidic ( $\text{pH} \leq 4$ ) and basic ( $\text{pH} > 7$ ) conditions while deswelling at moderate pH value (4–6) as shown in Fig. 9. In both conditions ( $\text{pH} \leq 4$  and  $\text{pH} > 7$ ), the structure has positive or negative charges in their network and repulsion takes place between the network of composite due to same charges. Therefore, the composite is present in a swelling state while at moderate pH (4–6), the structure of composite does not have any charge. Therefore, no repulsion occurs and composite present in deswelling state. During deswelling state, the metal sulfide can come out from the network of chitosan and showed greater photocatalytic degradation of dyes. For example, Li *et al.*<sup>41</sup> have synthesized cellulose-citric acid-chitosan@nickel sulfide (CL-CA-CS@NiS) and cellulose-citric acid-chitosan@copper sulfide (CL-CA-CS@CuS) nanocomposites and used them for degradation of MO. The degradation efficiency was obtained greater at moderate pH. 98.8% of MO was degraded at pH 6 while only 27.6% at pH 2 with CL-CA-CS@NiS at 35 °C in 120 min. Similarly, 93.4% of MO degradation was obtained by CL-CA-CS@CuS under similar conditions.

This dynamic pH-tunability of metal sulfide-chitosan composites offers significant advantages for selective pollutant targeting, wastewater with fluctuating pH conditions, and multi-component dye systems. Tailoring the structure of composite and functional group availability through controlled synthesis enables researchers to optimize performance for specific environmental applications. Therefore, pH responsiveness is not just a passive property but an actively tunable parameter for enhancing photocatalytic degradation mechanisms in real-world scenarios.

## 5.2. Temperature

The temperature of medium plays a crucial role in tuning their photocatalytic performance of metal sulfide-chitosan based composites, particularly under variable environmental or operational conditions. This thermo-responsiveness is largely governed by the physical and chemical adaptability of chitosan, which exhibits structural changes in response to temperature variations. Such temperature-induced transitions can significantly influence the diffusion of dye molecules, adsorption dynamics, charge carrier mobility, and catalytic stability.<sup>46</sup>

Polymeric matrix of chitosan undergoes conformational rearrangements at elevated temperatures, altering its porosity, hydrophilicity, and swelling characteristics. As temperature increases, the hydrogen bonding interactions between chitosan chains and water molecules are disrupted, leading to deswelling of the polymer network.<sup>102</sup> This thermally induced compaction



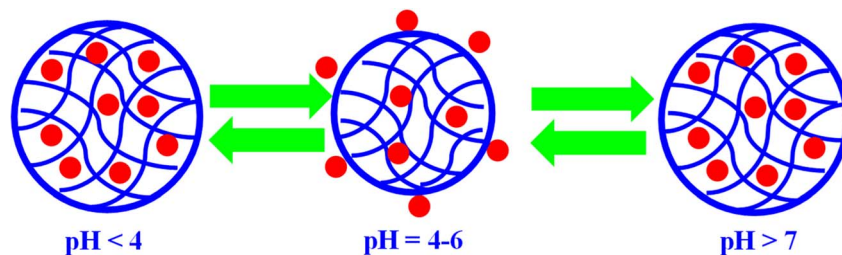


Fig. 9 pH effect on swelling behavior of carboxylic groups containing comonomer present in metal sulfide–chitosan composites.

may decrease the diffusion path length for dye molecules and ROS which improve their interaction with the photocatalytically active sites on the metal sulfide particles. Furthermore, increased temperature often enhances the kinetic energy of dye molecules, which can promote faster adsorption onto the composite surface, especially in thermodynamically favorable systems. Simultaneously, the elevated temperature may reduce charge recombination rates by promoting faster charge separation and transfer across the chitosan–metal sulfide interface. This is particularly relevant for sulfide semiconductors like ZnS, CdS, and MoS<sub>2</sub>, which often face limitations due to rapid electron–hole recombination under ambient conditions. Moreover, chitosan can act as a thermo-tolerant stabilizer and protects the metal sulfide nanoparticles from agglomeration or photo-corrosion at higher temperatures. This increases the thermal durability and reusability of the composite, making it suitable for long-term applications in wastewater treatment systems operating under fluctuating thermal environments.<sup>103</sup>

Modification of chitosan with temperature-sensitive moieties (e.g., grafting with poly(*N*-isopropylacrylamide) P(NIPAM) or similar thermos-responsive polymers), researchers can design smart nanocomposites that exhibit controlled adsorption, release, or catalytic activity above or below a specific transition temperature (lower critical solution temperature (LCST)). Such systems allow for the development of “on-demand” photocatalysts, which can be activated or deactivated by simple thermal triggers.

The temperature-responsive nature of metal sulfide–chitosan composites introduces a valuable dimension of control and adaptability in photocatalytic systems. It enables the fine-tuning of dye degradation rates, improves operational robustness, and paves the way for smart, stimuli-responsive materials in sustainable water purification technologies.

### 5.3. Light

The impact of light is central to their application in photocatalytic dye degradation by the metal sulfide–chitosan based composites, as the activation and efficiency of these materials are fundamentally dependent on light absorption and utilization. Metal sulfides like CdS, ZnS, MoS<sub>2</sub>, and CuS are known for their favorable band gaps in the visible region, which allow them to harness solar energy efficiently. When integrated with chitosan, their photo-reactivity is further modulated and often enhanced through improved light harvesting, charge transfer, and material stability.<sup>104</sup>

Chitosan plays multiple roles in enhancing the light responsiveness of these composites. First, it acts as a transparent and biocompatible matrix that does not hinder the penetration of light but instead facilitates the uniform dispersion of light-sensitive metal sulfide nanoparticles. This structural uniformity increases the surface-to-volume ratio which leads to more effective light absorption.<sup>68</sup> Additionally, chitosan can assist in band gap tuning when doped or functionalized, subtly modifying the electronic environment around the metal sulfide particles to improve visible light utilization. Moreover, chitosan can act as a photosensitizer or energy mediator, especially when conjugated with other light-active species such as dyes or carbon nanomaterials. This enables better charge excitation and transfer under visible or UV light. The synergistic interaction between chitosan and the metal sulfide components also promotes faster charge carrier mobility, reduces recombination rates, and enhances the generation of reactive oxygen species (ROS) like  $\cdot\text{OH}$  and  $\text{O}_2^{\cdot-}$ , which are critical for dye degradation.<sup>105</sup>

In smart photocatalytic systems, light can also be designed to be wavelength-selective or intensity-dependent which allow the composite to operate efficiently under natural sunlight or artificial light sources. This feature is especially valuable for designing on-demand or remote-activated photocatalytic devices in wastewater treatment, where precise control over the catalytic process is desirable.

The light-responsive nature of metal sulfide–chitosan based composites is a product of both the semiconducting properties of metal sulfides and the structural, electronic, and chemical contributions of chitosan. This responsiveness can be fine-tuned through morphological design, chemical modification, and hybrid engineering, enabling robust, sustainable, and efficient photocatalytic systems for environmental remediation.

### 5.4. Magnetic environment

The integration of magnetic components into metal sulfide–chitosan based composites introduces magnetic responsiveness, a highly valuable property for facilitating catalyst recovery, recyclability, and process control in photocatalytic applications. This behavior is typically imparted by incorporating magnetic nanoparticles like Fe<sub>3</sub>O<sub>4</sub> (magnetite) or  $\gamma\text{-Fe}_2\text{O}_3$  (maghemite) within the chitosan matrix along with metal sulfide photocatalysts such as CdS, ZnS, or MoS<sub>2</sub>. The resulting ternary or hybrid system retains the photocatalytic function of metal sulfides while gaining superparamagnetic characteristics,



Table 5 Summary of environmental impact of the photocatalytic activity of metal sulfide–chitosan based composites

Composites	Condition	Mechanism of response	Role of chitosan	Photocatalytic relevance	References
AgO–CS	pH	Protonation/deprotonation of amine and hydroxyl groups alters surface charge and binding	Provides pH-sensitive sites for selective adsorption of dyes	Enhances pollutant pre-concentration and facilitates pH-tuned degradation	69
NiS–CS	Temperature	Thermal impact on chitosan modulates porosity, surface area, and diffusion	Enables thermal effect in hydrogels or beads; enhances substrate access	Improves reaction kinetics and substrate-catalyst interactions at elevated temperatures	102
MoS <sub>2</sub> –NiFe <sub>2</sub> O <sub>4</sub> –CS	Light (visible/UV)	Excitation of metal sulfide generates e <sup>-</sup> /h <sup>+</sup> pairs; chitosan aids separation	Acts as electron reservoir, light-stabilizing matrix, and modulator of light penetration	Boosts ROS production, improves light absorption and charge separation efficiency	104
MoS <sub>2</sub> –CS–Fe <sub>3</sub> O <sub>4</sub>	Magnetic field	Magnetic nanoparticles (e.g., Fe <sub>3</sub> O <sub>4</sub> ) allow magnetic response; chitosan anchors them	Binds magnetic particles and sulfides simultaneously; offers structural integrity and recyclability	Allows magnetic separation, catalyst reuse without filtration	106

enabling easy separation from treated water using an external magnetic field.

Chitosan plays a critical role in stabilizing and uniformly distributing magnetic nanoparticles which prevent aggregation and maintain high surface area and dispersion of active sites. Its strong chelation ability with metal ions ensures robust immobilization of magnetic and photocatalytic particles, enhancing the durability and reusability of the composite. Additionally, the biopolymer matrix provides structural flexibility and surface functionality that can further modulate the interaction of the composite with dye molecules and reactive oxygen species during light irradiation.<sup>104</sup>

The magnetic responsiveness of these composites does not interfere with their photocatalytic performance but rather complements it by offering recyclability without centrifugation or filtration, thereby making the overall process more sustainable and economically viable. Studies have reported that magnetic-chitosan–metal sulfide composites retain high photocatalytic efficiency over multiple cycles, with minimal loss in activity, underscoring their potential for real-world wastewater treatment applications.<sup>106</sup>

The magnetic field-responsive nature also opens possibilities for magnetically targeted pollutant removal, enabling the controlled positioning of photocatalysts in flow systems or reactors. This functional versatility makes magnetic metal sulfide–chitosan composites a promising class of smart, recyclable materials in the field of environmental nanotechnology.

The summary of environmental impact the performance of metal sulfide–chitosan composites is provided in Table 5.

## 6. Conclusion and future directions

The integration of metal sulfides with chitosan-based matrices has led to the development of hybrid photocatalysts exhibiting improved performance in the degradation of organic dyes and

pollutants. These composites combine the visible-light responsiveness and semiconductor properties of metal sulfides (like FeS<sub>2</sub>, Bi<sub>2</sub>S<sub>3</sub>, ZnS, and CuS) with the biocompatibility, film-forming ability, and functional surface chemistry of chitosan. Chitosan not only enhances the dispersibility and stability of metal sulfide nanoparticles but also plays a crucial role in improving pollutant adsorption, facilitating charge separation, and suppressing photo-corrosion. These synergistic interactions result in enhanced photocatalytic degradation efficiency, selectivity, and recyclability, positioning metal sulfide–chitosan composites as promising materials for wastewater treatment and environmental remediation.

Several critical challenges remain to be addressed in the present study. One key area for future research is advanced band gap engineering through doping and heterojunction construction to extend light absorption into the visible and near-infrared range and improve quantum efficiency. Another important consideration is the development of non-toxic and environmentally benign metal sulfide alternatives like iron sulfide or bismuth sulfide to replace heavy-metal-based materials like CdS. Furthermore, modifying chitosan with additional functional groups can improve pollutant specificity and allow for multifunctional degradation systems that target multiple classes of contaminants. In terms of application, future studies should also focus on enhancing the structural integrity and recyclability of the composites under repeated cycles and long-term exposure to real wastewater conditions.

The scaling strategies such as fabricating chitosan–metal sulfide membranes, films, or beads are essential to transition from laboratory to field applications. This architecture allows easier handling and recovery compared to powders. Additionally, real-world testing using complex wastewater streams rather than model dyes should become a priority to better simulate environmental conditions. Innovations in reactor design and



solar harvesting systems can further improve light utilization and efficiency in practical settings. The integration of theoretical modeling and data-driven design approaches can also accelerate material optimization. Future progress in this field will depend on bridging material chemistry with process engineering which ultimately enables the widespread deployment of metal sulfide–chitosan photocatalysts for sustainable and effective pollutant degradation.

Morphological research has been rarely reported in literature. More research is required on the morphological characterization and their impact on their photocatalytic performance. The performance of core–shell systems will be different from homogenous photocatalyst and the position of photocatalyst in core–shell systems also indicate the effect of light and synergistic effect on photocatalytic activity. The corrosion of light can also be controlled in core–shell systems and hence control the performance. The heterojunction performance of two semiconductors will be different in core–shell systems than homogenous systems. These systems should be applied on industrial waste to identify real solutions for pollution of water. Therefore, deep research is required in this field in near future.

## Conflicts of interest

There is no conflict of interest.

## List of abbreviations

CS	Chitosan
NPs	Nanoparticles
MNPs	Metal nanoparticles
MS	Metal sulfide
MB	Methylene blue
CR	Congo red
CV	Crystal violet
MO	Methyl orange
RhB	Rhodamine-B
GO	Graphene oxide
rGO	Reduced graphene oxide
AB	Acid blue
ROS	Reactive oxygen species
LCST	Lower critical solution temperature
PAL	Polyacrylate
NIPAM	N-Isopropylacrylamide
CL	Cellulose
CA	Citric acid
NiS	Nickel sulfide
AO-VII	Acid orange-VII
AR-I	Acid red-I (AR-I)
IPN	Isopropanol (IPN)
BQ	Benzoquinone
SRB	Stimuli responsive behavior
AA	Ascorbic acid
AO-II	Acid orange-II
BBFCF	Brilliant blue FCF
AC	Activated carbon

VB	Valence band
CB	Conduction band
C	Carbon
Ag	Silver
Au	Gold
N	Nitrogen
ZnO	Zinc oxide
SPR	Surface plasmon resonance
UV-Vis	UV/visible spectroscopy
TiO <sub>2</sub>	Titanium dioxide
CdS	Cadmium sulfide
ZnS	Zinc sulfide
CuS	Copper sulfide
MoS <sub>2</sub>	Molybdenum disulfide

## Data availability

No primary research results, software or code have been included and no new data were generated or analysed as part of this review.

## Acknowledgements

Muhammad Arif is thankful to University of Management and Technology, Lahore-54770, Pakistan.

## References

- 1 A. P. Periyasamy, Textile Dyes in Wastewater and its Impact on Human and Environment: Focus on Bioremediation, *Water, Air, Soil Pollut.*, 2025, **236**(9), 1–39, DOI: [10.1007/S11270-025-08204-7](https://doi.org/10.1007/S11270-025-08204-7).
- 2 A. Gičević, L. Hindija and A. Karačić, Toxicity of azo dyes in pharmaceutical industry, *IFMBE Proc.*, 2020, **73**, 581–587, DOI: [10.1007/978-3-030-17971-7\\_88](https://doi.org/10.1007/978-3-030-17971-7_88).
- 3 M. C. Kannaujiya, R. Kumar, T. Mandal and M. K. Mondal, Experimental investigations of hazardous leather industry dye (Acid Yellow 2GL) removal from simulated wastewater using a promising integrated approach, *Process Saf. Environ. Prot.*, 2021, **155**, 444–454, DOI: [10.1016/J.PSEP.2021.09.040](https://doi.org/10.1016/J.PSEP.2021.09.040).
- 4 T. Bujak, M. Zagórska-dziok, A. Ziemlewska, Z. Nizioł-Łukaszewska, T. Wasilewski and Z. Hordyjewicz-Baran, Antioxidant and Cytoprotective Properties of Plant Extract from Dry Flowers as Functional Dyes for Cosmetic Products, *Molecules*, 2021, **26**, 2809–2826, DOI: [10.3390/MOLECULES26092809](https://doi.org/10.3390/MOLECULES26092809).
- 5 G. Shabir, M. Arif, A. Saeed and G. Hussain, Synthesis and Optical Study of Sensitive and Selective Calix[4] Based Cu<sup>2+</sup> Ion Detection Probes, *Russ. J. Gen. Chem.*, 2019, **89**(4), 813–818, DOI: [10.1134/S1070363219040285](https://doi.org/10.1134/S1070363219040285).
- 6 M. Arif, F. Tahir, A. Saeed, A. Mohyuddin and S. Nadeem, Synthesis and characterization of some new phloroglucinol based sensors and the effect of substituted functional groups on selectivity and sensitivity of sensors



- towards metal ions, *Chem. Data Collect.*, 2022, **41**, 100943, DOI: [10.1016/j.cdc.2022.100943](https://doi.org/10.1016/j.cdc.2022.100943).
- 7 Z. Rabbani, M. U. Khan, A. Anwar, G. Mustafa, A. U. Hassan and S. M. Alshehri, Pyrazine-Based Aromatic Dyes as Novel Photosensitizers with Improved Conduction Band and Photovoltaic Features: DFT Insights for Efficient Dye-Sensitized Solar Cells, *Polycycl. Aromat. Compd.*, 2025, **45**, 442–468, DOI: [10.1080/10406638.2024.2408462](https://doi.org/10.1080/10406638.2024.2408462).
  - 8 K. Wang, T. F. Lu, Y. Liang, Y. Wen, Y. Cui, H. Tao, M. He and Z. Zhang, Optimizing photovoltaic performance of D- $\pi$ -A-type organic dye: A DFT/TD-DFT study on promising aromatic heterocycles anchoring groups, *Mater. Sci. Semicond. Process.*, 2025, **192**, 109399, DOI: [10.1016/J.MSSP.2025.109399](https://doi.org/10.1016/J.MSSP.2025.109399).
  - 9 G. Venkatesan, H. Q. Yang, H. Chen, P. Bigliardi and G. Pastorin, Enhancement of detoxification of xenobiotic aromatic amine dyes by N-acetyltransferase 1 (NAT1) enzyme on human keratinocytes cells through structural modification, *Environ. Toxicol. Pharmacol.*, 2025, **114**, 104622, DOI: [10.1016/J.ETAP.2024.104622](https://doi.org/10.1016/J.ETAP.2024.104622).
  - 10 V. Ganthavee and A. P. Trzcinski, Superior decomposition of xenobiotic RB5 dye using three-dimensional electrochemical treatment: Response surface methodology modelling, artificial intelligence, and machine learning-based optimisation approaches, *Water Sci. Eng.*, 2025, **18**, 1–10, DOI: [10.1016/J.WSE.2024.05.003](https://doi.org/10.1016/J.WSE.2024.05.003).
  - 11 H. Kolya and C. W. Kang, Toxicity of Metal Oxides, Dyes, and Dissolved Organic Matter in Water: Implications for the Environment and Human Health, *Toxics*, 2024, **12**, 111, DOI: [10.3390/TOXICS12020111](https://doi.org/10.3390/TOXICS12020111).
  - 12 Y. Xu, K. Xu, Z. Wang, Y. Zhang, J. Chen, M. Zhao and J. Qiu, Highly stable Aza-BODIPY dyes for near-infrared-II PAI/FLI guided efficient tumor photothermal therapy, *Dyes Pigm.*, 2025, **243**, 113018, DOI: [10.1016/J.DYEPIG.2025.113018](https://doi.org/10.1016/J.DYEPIG.2025.113018).
  - 13 J. Rovira, M. C. O. Souza, M. Nadal and J. L. Domingo, Human health risks from textile chemicals: a critical review of recent evidence (2019–2025), *J. Environ. Sci. Health, Part A: Toxic/Hazard. Subst. Environ. Eng.*, 2025, **60**, 79–91, DOI: [10.1080/10934529.2025.2514406](https://doi.org/10.1080/10934529.2025.2514406).
  - 14 A. Bhava, U. S. Shenoy and D. K. Bhat, Silver doped barium titanate nanoparticles for enhanced visible light photocatalytic degradation of dyes, *Environ. Pollut.*, 2024, **344**, 123430, DOI: [10.1016/J.ENVPOL.2024.123430](https://doi.org/10.1016/J.ENVPOL.2024.123430).
  - 15 A. Aziz, N. Ali, A. Khan, M. Bilal, S. Malik, N. Ali and H. Khan, Chitosan-zinc sulfide nanoparticles, characterization and their photocatalytic degradation efficiency for azo dyes, *Int. J. Biol. Macromol.*, 2020, **153**, 502–512, DOI: [10.1016/J.IJBIOMAC.2020.02.310](https://doi.org/10.1016/J.IJBIOMAC.2020.02.310).
  - 16 M. Arif, M. Javed and T. Akhter, Crosslinked polymeric networks of TiO<sub>2</sub>–polymer composites: a comprehensive review, *RSC Adv.*, 2024, **14**, 33843–33863, DOI: [10.1039/D4RA06922F](https://doi.org/10.1039/D4RA06922F).
  - 17 M. Arif, A. Rauf and T. Akhter, A comprehensive review on crosslinked network systems of zinc oxide-organic polymer composites, *Int. J. Biol. Macromol.*, 2024, **274**, 133250, DOI: [10.1016/J.IJBIOMAC.2024.133250](https://doi.org/10.1016/J.IJBIOMAC.2024.133250).
  - 18 H. M. Rasheed, A. Rauf, M. Arif, A. Mohyuddin, M. Javid, S. Nadeem, A. Yousuf, M. Irfan, S. M. Haroon, H. Raza, S. M. Ibrahim and S. U. Mahmood, Selective Removal of Lead (II) Ions from Wastewater with Fabricated ZnO-PVA Membrane, *JOM*, 2023, **75**, 5310–5320, DOI: [10.1007/S11837-023-05957-6](https://doi.org/10.1007/S11837-023-05957-6).
  - 19 C. Cheng, D. Bao, S. Sun, Y. Zhou, L. Tian, B. Zhang, Y. Yu, J. Guo and S. Zhang, Chitosan/copper sulfide nanoparticles (CS/CuSNPs) hybrid fibers with improved mechanical and photo-thermal conversion properties via tuning CuSNPs' morphological structures, *Int. J. Biol. Macromol.*, 2023, **253**, 127098, DOI: [10.1016/J.IJBIOMAC.2023.127098](https://doi.org/10.1016/J.IJBIOMAC.2023.127098).
  - 20 T. N. Krishna, B. V. Tirupanyam and M. S. Laxmi, Hydrothermal fabrication of ZnS/chitosan composite for effective photocatalytic degradation of Eosin blue and inactivation of bacterial pathogens, *J. Mater. Sci.*, 2025, **60**(41), 19755–19769, DOI: [10.1007/S10853-025-11612-Z](https://doi.org/10.1007/S10853-025-11612-Z).
  - 21 J. Hou, L. Guo, B. Yan, S. Gao, C. Sun, Y. Xu and Q. Wang, Study on LC wireless passive humidity sensor using MoS<sub>2</sub>/CS composite material: examination of high sensitivity and the chemical-physical synergistic adsorption mechanism, *Measurement*, 2026, **257**, 118825, DOI: [10.1016/J.MEASUREMENT.2025.118825](https://doi.org/10.1016/J.MEASUREMENT.2025.118825).
  - 22 A. Mandal, A. Poongan, E. Dhineshkumar and E. Murugan, Effect of Sago Starch on CuO Nanorods Impregnated in the Soy Protein Matrix: A Green Approach Using the Cytosine Molecule as an Electrochemical Sensor for Pharmaceuticals, *ACS Appl. Eng. Mater.*, 2023, **1**, 2137–2152, DOI: [10.1021/ACSAENM.3C00261](https://doi.org/10.1021/ACSAENM.3C00261).
  - 23 A. Mandal, E. Dhineshkumar and E. Murugan, Collagen Biocomposites Derived from Fish Waste: Doped and Cross-Linked with Functionalized Fe<sub>3</sub>O<sub>4</sub> Nanoparticles and Their Comparative Studies with a Green Approach, *ACS Omega*, 2023, **8**, 24256–24267, DOI: [10.1021/ACSOMEGA.3C01106](https://doi.org/10.1021/ACSOMEGA.3C01106).
  - 24 A. Mandal, E. Dhineshkumar and T. P. Sastry, The CCLW collagen biocomposite consisting Ag–Fe<sub>3</sub>O<sub>4</sub> nanoparticles as a novel biomaterial with a view to facile green approach, *Clean Technol. Environ. Policy*, 2023, **25**(10), 3285–3302, DOI: [10.1007/S10098-023-02578-0](https://doi.org/10.1007/S10098-023-02578-0).
  - 25 M. M. H. Farahani, M. Hajiebrahimi, S. Alamdari, A. Najafzadehkhoe, G. M. Khounsaraki, M. Agheb, V. Kostiuik, A. Puškárová, M. Bučková, D. Pangallo, P. Hvizdoš and O. Mirzaee, Synthesis and antibacterial activity of silver doped zinc sulfide/chitosan bionanocomposites: A new frontier in biomedical applications, *Int. J. Biol. Macromol.*, 2024, **280**, 135934, DOI: [10.1016/J.IJBIOMAC.2024.135934](https://doi.org/10.1016/J.IJBIOMAC.2024.135934).
  - 26 M. M. Hosseinieh Farahani, M. Hajiebrahimi, A. H. Afzali, D. Moradi, S. Alamdari and O. Mirzaee, Exploring the Antibacterial Potential of Zinc Sulfide/Chitosan Nanocomposites, *Adv. Ceram. Prog.*, 2025, **11**, 19–27, DOI: [10.30501/ACP.2025.486319.1164](https://doi.org/10.30501/ACP.2025.486319.1164).
  - 27 H. Wang, R. Liu, Q. Chen, H. Xia and Y. Zhang, Novel Chitosan-FeS@biochar-added constructed wetland microcosms for NH<sub>4</sub><sup>+</sup>/NO<sub>3</sub><sup>-</sup> and Pb removal: Performance



- and mechanism, *J. Environ. Chem. Eng.*, 2023, **11**, 110400, DOI: [10.1016/J.JECE.2023.110400](https://doi.org/10.1016/J.JECE.2023.110400).
- 28 J. Wu, Y. Zhao, J. Dai, B. Yang, Y. Zhang and X. Pu, Removal of hexavalent chromium from aqueous by Chitosan-stabilized FeS, *Water Energy Nexus*, 2023, **6**, 64–73, DOI: [10.1016/J.WEN.2023.07.003](https://doi.org/10.1016/J.WEN.2023.07.003).
- 29 Y. Han, J. Tao, A. Khan, R. Ullah, N. Ali, N. Ali, S. Malik, C. Yu, Y. Yang and M. Bilal, Design and fabrication of chitosan cross-linked bismuth sulfide nanoparticles for sequestration of mercury in river water samples, *Environ. Res.*, 2022, **215**, 113978, DOI: [10.1016/J.ENVRES.2022.113978](https://doi.org/10.1016/J.ENVRES.2022.113978).
- 30 O. V. Uhuo, K. C. Januarie, K. V. Mokwebo, M. Oranzie, M. Cox, J. L. January, Z. D. Leve, N. A. Sanga and E. I. Iwuoha, Trimetallic Chalcogenide-Sensitised Interferon Gamma Aptasensor For Tuberculosis, *Electrochim. Acta*, 2025, 146848, DOI: [10.1016/J.ELECTACTA.2025.146848](https://doi.org/10.1016/J.ELECTACTA.2025.146848).
- 31 N. Maghami and M. Mokhtary, Preparation and Characterization of Silver Sulfide Nanoparticle (Ag 2 S)-Coated Chitosan for the Delivery Of Methotrexate, *Drug Deliv. Lett.*, 2024, **15**, 46–57, DOI: [10.2174/0122103031300746240823094335](https://doi.org/10.2174/0122103031300746240823094335).
- 32 A. S. Eltaweil, N. Al Harby, M. El Batouti and E. M. Abd El-Monaem, Engineering a sustainable cadmium sulfide/polyethyleneimine-functionalized biochar/chitosan composite for effective chromium adsorption: optimization, co-interfering anions, and mechanisms, *RSC Adv.*, 2024, **14**, 22266–22279, DOI: [10.1039/D4RA03479A](https://doi.org/10.1039/D4RA03479A).
- 33 H. Wu, Y. Liu, B. Chen, F. Yang, L. Wang, Q. Kong, T. Ye and J. Lian, Enhanced adsorption of molybdenum(VI) from aquatic solutions by chitosan-coated zirconium-iron sulfide composite, *Sep. Purif. Technol.*, 2021, **279**, 119736, DOI: [10.1016/J.SEPPUR.2021.119736](https://doi.org/10.1016/J.SEPPUR.2021.119736).
- 34 P. Guo, X. Gu, Z. Li, X. Xu, Y. Cao, G. Yang, C. Kuang, X. Li, Y. Qing and Y. Wu, A novel almond shell biochar modified with FeS and chitosan as adsorbents for mitigation of heavy metals from water and soil, *Sep. Purif. Technol.*, 2025, **360**, 130943, DOI: [10.1016/J.SEPPUR.2024.130943](https://doi.org/10.1016/J.SEPPUR.2024.130943).
- 35 S. N. Rajakumari, R. B. Suneetha and C. Vedhi, Enhanced Supercapacitance Behaviours of Copper-Cobalt sulfide/reduced graphene Oxide/Chitosan ternary Econanocomposite, *Inorg. Chem. Commun.*, 2025, **172**, 113655, DOI: [10.1016/J.INOCHE.2024.113655](https://doi.org/10.1016/J.INOCHE.2024.113655).
- 36 J. Guo, H. Ma, H. Shang, W. Wang, R. Yang, S. Wang, Y. Miao, D. L. Phillips, G. Li and S. Xiao, Dual-site Langmuir-Hinshelwood mechanism in ZnCr-LDH/NH<sub>2</sub>-UIO66 heterojunction for efficient photocatalytic NO oxidation, *J. Hazard. Mater.*, 2025, **492**, 138060, DOI: [10.1016/J.JHAZMAT.2025.138060](https://doi.org/10.1016/J.JHAZMAT.2025.138060).
- 37 L. Liu, H. Song, S. Zhao, H. Zhang, P. Chen, J. Wu, F. Jia and S. Song, Nanoarchitectonics of CoS<sub>2</sub>/MoS<sub>2</sub>@chitosan aerogel as a peroxydisulfate activator for tetracycline degradation under light irradiation, *J. Environ. Chem. Eng.*, 2024, **12**, 113589, DOI: [10.1016/J.JECE.2024.113589](https://doi.org/10.1016/J.JECE.2024.113589).
- 38 S. Malik, A. Khan, H. Rahim, S. Rahim, A. Munawar, N. Ali, M. Bououdina, A. Nawaz and N. Ali, Biodegradable cobalt and tin doped chitosan nanocomposites from structure tailoring to solar-driven photocatalytic degradation of toxic organic dyes, *Int. J. Biol. Macromol.*, 2024, **283**, 137512, DOI: [10.1016/J.IJBIOMAC.2024.137512](https://doi.org/10.1016/J.IJBIOMAC.2024.137512).
- 39 I. Risha Achaiah, B. H. Gayathri, N. Banu, C. S. Kaliprasad, B. N. Beena ullala mata, K. P. Ajeya, K. Balakrishna, Udayabhanu, K. Prashantha, Y. R. Girish and S. M. Anush, Efficient removal of metal ions from aqueous solutions using MoS<sub>2</sub> functionalized chitosan Schiff base incorporated with Fe<sub>3</sub>O<sub>4</sub> nanoparticle, *Int. J. Biol. Macromol.*, 2023, **248**, 125976, DOI: [10.1016/J.IJBIOMAC.2023.125976](https://doi.org/10.1016/J.IJBIOMAC.2023.125976).
- 40 M. Hosseini, A. Pourabadeh, A. Fakhri, J. Hallajzadeh and S. Tahami, Synthesis and characterization of Sb<sub>2</sub>S<sub>3</sub>-CeO<sub>2</sub>/chitosan-starch as a heterojunction catalyst for photo-degradation of toxic herbicide compound: Optical, photo-reusable, antibacterial and antifungal performances, *Int. J. Biol. Macromol.*, 2018, **118**, 2108–2112, DOI: [10.1016/J.IJBIOMAC.2018.07.065](https://doi.org/10.1016/J.IJBIOMAC.2018.07.065).
- 41 J. Li, Q. Zhang, B. Chen, F. Li and C. Pang, Cellulose-citric acid-chitosan@metal sulfide nanocomposites: Methyl orange dye removal and antibacterial activity, *Int. J. Biol. Macromol.*, 2024, **276**, 133795, DOI: [10.1016/J.IJBIOMAC.2024.133795](https://doi.org/10.1016/J.IJBIOMAC.2024.133795).
- 42 H. Lin, T. Li, B. J. Janani and A. Fakhri, Fabrication of Cu<sub>2</sub>MoS<sub>4</sub> decorated WO<sub>3</sub> nano heterojunction embedded on chitosan: Robust photocatalytic efficiency, antibacterial performance, and bacteria detection by peroxidase activity, *J. Photochem. Photobiol., B*, 2022, **226**, 112354, DOI: [10.1016/J.JPHOTOBIO.2021.112354](https://doi.org/10.1016/J.JPHOTOBIO.2021.112354).
- 43 S. Sheshmani and M. Mardali, Harnessing the Synergistic Potential of ZnS Nanoparticle-Interfacing Chitosan for Enhanced Photocatalytic Degradation in Aqueous Media and Textile Wastewater, *J. Polym. Environ.*, 2024, **32**, 5783–5805, DOI: [10.1007/S10924-024-03307-4](https://doi.org/10.1007/S10924-024-03307-4).
- 44 R. K. V. Chola, S. Palliyalil, V. Sivakumar and B. M. Chelaveetil, Hydrothermally modified rice husk derived silica and molybdenum sulphide embedded chitosan matrix for the removal of cationic dyes, *Int. J. Biol. Macromol.*, 2025, **306**, 141465, DOI: [10.1016/J.IJBIOMAC.2025.141465](https://doi.org/10.1016/J.IJBIOMAC.2025.141465).
- 45 S. Sheshmani and M. Mirhabibi, Interfacial approach in CdS/chitosan based on reduced graphene oxide: co-doping, synergistic effects and enhancing dye degradation efficiency, *Chem. Pap.*, 2024, **78**, 4455–4468, DOI: [10.1007/S11696-024-03409-2](https://doi.org/10.1007/S11696-024-03409-2).
- 46 S. Wang, H. Wang, S. Wang, L. Zhang and L. Fu, Highly effective and selective adsorption of Au(III) from aqueous solution by poly(ethylene sulfide) functionalized chitosan: Kinetics, isothermal adsorption and thermodynamics, *Microporous Mesoporous Mater.*, 2022, **341**, 112074, DOI: [10.1016/J.MICROMESO.2022.112074](https://doi.org/10.1016/J.MICROMESO.2022.112074).
- 47 A. Sobhani, Nickel and Cadmium Sulfide/Chitosan Nanocomposites: Synthesis, Characterization and



- Applications, *J. Nanostruct.*, 2023, **13**, 902–914, DOI: [10.22052/JNS.2023.04.001](https://doi.org/10.22052/JNS.2023.04.001).
- 48 S. Roy, A. Mondal, V. Yadav, A. Sarkar, R. Banerjee, P. Sanpui and A. Jaiswal, Mechanistic Insight into the Antibacterial Activity of Chitosan Exfoliated MoS<sub>2</sub> Nanosheets: Membrane Damage, Metabolic Inactivation, and Oxidative Stress, *ACS Appl. Bio Mater.*, 2019, **2**, 2738–2755, DOI: [10.1021/ACSABM.9B00124](https://doi.org/10.1021/ACSABM.9B00124).
- 49 F. Jamal, A. Rafique, S. Moeen, J. Haider, W. Nabgan, A. Haider, M. Imran, G. Nazir, M. Alhassan, M. Ikram, Q. Khan, G. Ali, M. Khan, W. Ahmad and M. Maqbool, Review of Metal Sulfide Nanostructures and their Applications, *ACS Appl. Nano Mater.*, 2023, **6**(9), 7077–7106, DOI: [10.1021/ACSANM.3C00417](https://doi.org/10.1021/ACSANM.3C00417).
- 50 Q. Zhu, Q. Xu, M. Du, X. Zeng, G. Zhong, B. Qiu and J. Zhang, Recent Progress of Metal Sulfide Photocatalysts for Solar Energy Conversion, *Adv. Mater.*, 2022, **34**, 2202929, DOI: [10.1002/ADMA.202202929](https://doi.org/10.1002/ADMA.202202929).
- 51 M. Arif, A review on advanced research of combine life of polystyrene (hard) and organic polymer (soft) materials: from 2018 to present, *Z. Phys. Chem.*, 2023, **237**, 809–843, DOI: [10.1515/ZPCH-2022-0142](https://doi.org/10.1515/ZPCH-2022-0142).
- 52 M. Arif, Exploring microgel adsorption: synthesis, classification, and pollutant removal dynamics, *RSC Adv.*, 2024, **14**, 9445–9471, DOI: [10.1039/D4RA00563E](https://doi.org/10.1039/D4RA00563E).
- 53 M. Arif, Core-shell systems of crosslinked organic polymers: A critical review, *Eur. Polym. J.*, 2024, **206**, 112803, DOI: [10.1016/J.EURPOLYMJ.2024.112803](https://doi.org/10.1016/J.EURPOLYMJ.2024.112803).
- 54 M. Arif, Catalytic reduction/degradation of methyl orange by metal nanoparticle containing systems: a critical review, *RSC Adv.*, 2025, **15**, 27668–27684, DOI: [10.1039/D5RA04059K](https://doi.org/10.1039/D5RA04059K).
- 55 M. Arif, Adsorptive removal and photocatalytic degradation of tartrazine: A critical review, *J. Alloys Compd.*, 2025, **1046**, 184820, DOI: [10.1016/J.JALLCOM.2025.184820](https://doi.org/10.1016/J.JALLCOM.2025.184820).
- 56 K. Naseem, E. Abrar, A. Khalid and M. A. Ismail, Inorganic nanoparticles as a potential catalyst for the reduction of Rhodamine B dye: A critical review, *Inorg. Chem. Commun.*, 2024, **163**, 112367, DOI: [10.1016/J.INOCHE.2024.112367](https://doi.org/10.1016/J.INOCHE.2024.112367).
- 57 C. Yuan, Q. Liu, M. Wei, S. Zhao, X. Yang, B. Cao, S. Wang, A. El-Fatah Abomohra, X. Liu and Y. Hu, Selective oxidation of 5-hydroxymethylfurfural to furan-2,5-dicarbaldehyde using chitosan-based biochar composite cadmium sulfide quantum dots, *Fuel*, 2022, **320**, 123994, DOI: [10.1016/J.FUEL.2022.123994](https://doi.org/10.1016/J.FUEL.2022.123994).
- 58 S. Bose, S. A. Razack, S. Arthanari, Y. Kim, H. Lee and H. W. Kang, Near-infrared light-responsive Cu<sub>2</sub>O@CuFeS<sub>2</sub>-hydroxyapatite-chitosan based antibacterial coating on titanium bioimplant, *Prog. Org. Coat.*, 2023, **183**, 107714, DOI: [10.1016/J.PORGCOAT.2023.107714](https://doi.org/10.1016/J.PORGCOAT.2023.107714).
- 59 B. Luo, J. Cai, Y. Xiong, X. Ding, X. Li, S. Li, C. Xu, A. Y. Vasil'kov, Y. Bai and X. Wang, Quaternized chitosan coated copper sulfide nanozyme with peroxidase-like activity for synergistic antibacteria and promoting infected wound healing, *Int. J. Biol. Macromol.*, 2023, **246**, 125651, DOI: [10.1016/J.IJBIOMAC.2023.125651](https://doi.org/10.1016/J.IJBIOMAC.2023.125651).
- 60 G. Y. Huang, W. J. Chang, T. W. Lu, I. L. Tsai, S. J. Wu, M. H. Ho and F. L. Mi, Electrospun CuS nanoparticles/chitosan nanofiber composites for visible and near-infrared light-driven catalytic degradation of antibiotic pollutants, *Chem. Eng. J.*, 2022, **431**, 134059, DOI: [10.1016/J.CEJ.2021.134059](https://doi.org/10.1016/J.CEJ.2021.134059).
- 61 A. Fakhri, V. K. Gupta, H. Rabizadeh, S. Agarwal, N. Sadeghi and S. Tahami, Preparation and characterization of WS<sub>2</sub> decorated and immobilized on chitosan and polycaprolactone as biodegradable polymers nanofibers: Photocatalysis study and antibiotic-conjugated for antibacterial evaluation, *Int. J. Biol. Macromol.*, 2018, **120**, 1789–1793, DOI: [10.1016/J.IJBIOMAC.2018.09.207](https://doi.org/10.1016/J.IJBIOMAC.2018.09.207).
- 62 B. Janani, M. K. Okla, M. A. Abdel-Maksoud, H. AbdElgawad, A. M. Thomas, L. L. Raju, W. H. Al-Qahtani and S. S. Khan, CuO loaded ZnS nanoflower entrapped on PVA-chitosan matrix for boosted visible light photocatalysis for tetracycline degradation and antibacterial application, *J. Environ. Manage.*, 2022, **306**, 114396, DOI: [10.1016/J.JENVMAN.2021.114396](https://doi.org/10.1016/J.JENVMAN.2021.114396).
- 63 L. Rani and R. P. Chauhan, Effect of Reaction Temperature on the Properties of Mesoporous CdS/ZnS Heterostructure Nanocomposites for Efficient Antibacterial Applications, *ChemistrySelect*, 2025, **10**, e01596, DOI: [10.1002/SLCT.202501596](https://doi.org/10.1002/SLCT.202501596).
- 64 W. Dai, C. Wang, Y. Wang, J. Sun, H. Ruan, Y. Xue and S. Xiao, Unlocking photocatalytic NO removal potential in an S-type UiO-66-NH<sub>2</sub>/ZnS(en)<sub>0.5</sub> heterostructure, *Interdiscip. Mater.*, 2024, **3**, 400–413, DOI: [10.1002/IDM2.12160](https://doi.org/10.1002/IDM2.12160).
- 65 M. Y. Heng, H. L. Shao, J. T. Sun, Q. Huang, S. L. Shen, G. Z. Yang, Y. H. Xue and S. N. Xiao, Harnessing S-scheme junctions for enhanced CO<sub>2</sub> photoreduction: molecular bonding of copper(II) complexes onto K-doped polymeric carbon nitride via microwave heating, *Rare Met.*, 2024, **44**(2), 1108–1121, DOI: [10.1007/S12598-024-03000-4](https://doi.org/10.1007/S12598-024-03000-4).
- 66 I. Chuasontia, B. Tangnorawich, O. Pechtes, N. Nakpathomkun, C. Pechyen and Y. Parcharoen, Fabrication composite of copper sulfide nanoparticles/multiwall carbon nanotubes stabilized by chitosan modified screen-printed carbon electrode: Sensitive analysis of the paraoxon ethyl, *Sens. Bio-Sens. Res.*, 2025, **49**, 100819, DOI: [10.1016/J.SBSR.2025.100819](https://doi.org/10.1016/J.SBSR.2025.100819).
- 67 Z. Liu, D. Bao, S. Jia, J. Qiao, D. Xiang, H. Li, L. Tian, B. Zhang, X. Zhang, H. Zhang, J. Guo and S. Zhang, The regulation of CuSNPs' interface for further enhancing mechanical and photothermal conversion properties of chitosan/@CuSNPs hybrid fibers, *Int. J. Biol. Macromol.*, 2024, **265**, 130931, DOI: [10.1016/J.IJBIOMAC.2024.130931](https://doi.org/10.1016/J.IJBIOMAC.2024.130931).
- 68 S. Muthuvijayan, R. K. Manavalan, J. S. Ponraj, S. Balasubramanian, S. C. B. Gopinath and T. Theivasanthi, Chitosan-mediated tailoring of cadmium sulphide nanoparticle: Synthesis, properties, and



- interactive mechanisms, *Process Biochem.*, 2024, **144**, 38–44, DOI: [10.1016/J.PROCBIO.2024.05.014](https://doi.org/10.1016/J.PROCBIO.2024.05.014).
- 69 K. Vijayan and S. P. Vijayachamundeswari, Effect of Chitosan on the Optical Properties of Facile Co-Precipitation Route-Prepared Silver Sulfide Nanoparticles, *J. Polym. Environ.*, 2023, **31**, 3272–3281, DOI: [10.1007/S10924-023-02814-0](https://doi.org/10.1007/S10924-023-02814-0).
- 70 A. Jbeli, A. M. Ferraria, A. M. Botelho do Rego, S. Boufi and S. Bouattour, Hybrid chitosan-TiO<sub>2</sub>/ZnS prepared under mild conditions with visible-light driven photocatalytic activity, *Int. J. Biol. Macromol.*, 2018, **116**, 1098–1104, DOI: [10.1016/J.IJBIOMAC.2018.05.141](https://doi.org/10.1016/J.IJBIOMAC.2018.05.141).
- 71 B. A. Bhat, N. Jadon, L. Dubey and S. A. Mir, Facile Synthesis of a Crystalline Zinc Sulfide/Chitosan Biopolymer Nanocomposite: Characterization and Application for Photocatalytic Degradation of Textile Dyes and Anticancer Activity, *ACS Omega*, 2024, **9**, 24425–24437, DOI: [10.1021/ACSOMEGA.4C00247](https://doi.org/10.1021/ACSOMEGA.4C00247).
- 72 Y. Zhang, W. Zhou, J. Wang, L. Jia, L. Liu, X. Tan, T. Yu and J. Ye, Hydrated electrons mediated in-situ construction of cubic phase CdS/Cd thin layer on a millimeter-scale support for photocatalytic hydrogen evolution, *J. Colloid Interface Sci.*, 2022, **607**, 769–781, DOI: [10.1016/J.JCIS.2021.09.039](https://doi.org/10.1016/J.JCIS.2021.09.039).
- 73 X. Li, Z. Zhang, A. Fakhri, V. K. Gupta and S. Agarwal, Adsorption and photocatalysis assisted optimization for drug removal by chitosan-glyoxal/Polyvinylpyrrolidone/MoS<sub>2</sub> nanocomposites, *Int. J. Biol. Macromol.*, 2019, **136**, 469–475, DOI: [10.1016/J.IJBIOMAC.2019.06.003](https://doi.org/10.1016/J.IJBIOMAC.2019.06.003).
- 74 J. Wang, J. Sun, J. Huang, A. Fakhri and V. K. Gupta, Synthesis and its characterization of silver sulfide/nickel titanate/chitosan nanocomposites for photocatalysis and water splitting under visible light, and antibacterial studies, *Mater. Chem. Phys.*, 2021, **272**, 124990, DOI: [10.1016/J.MATCHEMPHYS.2021.124990](https://doi.org/10.1016/J.MATCHEMPHYS.2021.124990).
- 75 K. C. Monyake and L. Alagha, Enhanced separation of base metal sulfides in flotation systems using Chitosan-grafted-Polyacrylamides, *Sep. Purif. Technol.*, 2022, **281**, 119818, DOI: [10.1016/J.SEPPUR.2021.119818](https://doi.org/10.1016/J.SEPPUR.2021.119818).
- 76 T. A. Afolabi, O. Ejeromedoghene, O. T. Akinbile, T. A. Afolabi, R. C. Ebubekukwu and O. O. Ogundiran, Chitosan-thymolsulfonephthalein-cobalt nanocomposites for colorimetric detection of sulfide anions in aqueous solution, *J. Trace Elem. Min.*, 2023, **4**, 100055, DOI: [10.1016/J.JTEMIN.2023.100055](https://doi.org/10.1016/J.JTEMIN.2023.100055).
- 77 T. Feng, T. Zhao, L. Xu and B. Deng, Photocatalytic degradation of methyl orange by chitosan/CdS nanoparticle composite films, *Desalination Water Treat.*, 2017, **60**, 242–248, DOI: [10.5004/DWT.2017.1482](https://doi.org/10.5004/DWT.2017.1482).
- 78 M. Kiani, M. Bagherzadeh, R. Kaveh, N. Rabiee, Y. Fatahi, R. Dinarvand, H. W. Jang, M. Shokouhimehr and R. S. Varma, Novel Pt-Ag<sub>3</sub>PO<sub>4</sub>/CdS/Chitosan Nanocomposite with Enhanced Photocatalytic and Biological Activities, *Nanomaterials*, 2020, **10**, 2320, DOI: [10.3390/NANO10112320](https://doi.org/10.3390/NANO10112320).
- 79 H. Pan, H. Xie, G. Chen, N. Xu, M. Wang and A. Fakhri, Cr<sub>2</sub>S<sub>3</sub>-Co<sub>3</sub>O<sub>4</sub> on polyethylene glycol-chitosan nanocomposites with enhanced ultraviolet light photocatalysis activity, antibacterial and antioxidant studies, *Int. J. Biol. Macromol.*, 2020, **148**, 608–614, DOI: [10.1016/J.IJBIOMAC.2019.12.262](https://doi.org/10.1016/J.IJBIOMAC.2019.12.262).
- 80 M. A. Ahmed, M. Farag, M. A. Ahmed, S. A. Mahmoud and A. A. Mohamed, Enhancing the adsorption capacity of SnS<sub>2</sub>-g-C<sub>3</sub>N<sub>4</sub> through chitosan integration: Insights from structural and optical characterization, *Surf. Interfaces*, 2025, **64**, 106321, DOI: [10.1016/J.SURFIN.2025.106321](https://doi.org/10.1016/J.SURFIN.2025.106321).
- 81 T. Xaba, J. Magagula and O. B. Nchoe, “Green” synthesis of Cu<sub>2</sub>S nanoparticles from (Z)-1-methyl-2-(pyrrolidin-2-ylidene)thiourea ligand for the preparation of Cu<sub>2</sub>S-chitosan nanocomposites for the removal of Cr(VI) ion from wastewater, *Mater. Lett.*, 2018, **229**, 331–335, DOI: [10.1016/J.MATLET.2018.07.057](https://doi.org/10.1016/J.MATLET.2018.07.057).
- 82 Z. Cao, X. Kang, W. Lü and W. Guan, Direct synthesis of eco-friendly carboxymethyl chitosan functionalized AgInS<sub>2</sub>/ZnS quantum dots: Utilization in ink and flexible film, warm-white LED, NIR-LED and counterfeit prevention, *J. Alloys Compd.*, 2025, **1022**, 179801, DOI: [10.1016/J.JALLCOM.2025.179801](https://doi.org/10.1016/J.JALLCOM.2025.179801).
- 83 C. Nong, B. Yang, X. Li, S. Feng and H. Cui, An ultrasensitive electrochemical immunosensor based on in-situ growth of CuWO<sub>4</sub> nanoparticles on MoS<sub>2</sub> and chitosan-gold nanoparticles for cortisol detection, *Microchem. J.*, 2022, **179**, 107434, DOI: [10.1016/J.MICROC.2022.107434](https://doi.org/10.1016/J.MICROC.2022.107434).
- 84 D. Wang, W. Chang, Z. Ren, X. Zhang, Y. Du, B. Liu and Y. Li, Low-temperature hydrothermal self-assembly synthesis of ZnIn<sub>2</sub>S<sub>4</sub>/chitosan-graphene aerogels for enhanced aqueous pollutants removal, *Vacuum*, 2024, **230**, 113736, DOI: [10.1016/J.VACUUM.2024.113736](https://doi.org/10.1016/J.VACUUM.2024.113736).
- 85 V. Gadore, S. R. Mishra and M. Ahmaruzzaman, Green and environmentally sustainable fabrication of SnS<sub>2</sub> quantum dots/chitosan nanocomposite for enhanced photocatalytic performance: Effect of process variables, and water matrices, *J. Hazard. Mater.*, 2023, **444**, 130301, DOI: [10.1016/J.JHAZMAT.2022.130301](https://doi.org/10.1016/J.JHAZMAT.2022.130301).
- 86 J. Lin, D. Gao, J. Zeng, Z. Li, Z. Wen, F. Ke, Z. Xia and D. Wang, MXene/ZnS/chitosan-cellulose composite with Schottky heterostructure for efficient removal of anionic dyes by synergistic effect of adsorption and photocatalytic degradation, *Int. J. Biol. Macromol.*, 2024, **269**, 131994, DOI: [10.1016/J.IJBIOMAC.2024.131994](https://doi.org/10.1016/J.IJBIOMAC.2024.131994).
- 87 G. Wang and A. Fakhri, Preparation of CuS/polyvinyl alcohol-chitosan nanocomposites with photocatalysis activity and antibacterial behavior against G<sup>+</sup>/G<sup>-</sup> bacteria, *Int. J. Biol. Macromol.*, 2020, **155**, 36–41, DOI: [10.1016/J.IJBIOMAC.2020.03.077](https://doi.org/10.1016/J.IJBIOMAC.2020.03.077).
- 88 B. Luo, X. Li, P. Liu, M. Cui, G. Zhou, J. Long and X. Wang, Self-assembled NIR-responsive MoS<sub>2</sub>@quaternized chitosan/nanocellulose composite paper for recyclable antibacteria, *J. Hazard. Mater.*, 2022, **434**, 128896, DOI: [10.1016/J.JHAZMAT.2022.128896](https://doi.org/10.1016/J.JHAZMAT.2022.128896).
- 89 M. Ikram, H. Maghfoor, A. Shahzadi, A. Haider, I. Shahzadi, N. Abid, A. Ul-Hamid, J. Haider, W. Nabgan and A. R. Butt, Towards effective dye degradation and antimicrobial behavior of chitosan and C<sub>3</sub>N<sub>4</sub>-doped CdS nanoparticles,



- Mater. Today Commun.*, 2022, **33**, 104814, DOI: [10.1016/J.MTCOMM.2022.104814](https://doi.org/10.1016/J.MTCOMM.2022.104814).
- 90 D. E. Al Momani, F. Arshad and L. Zou, Chitosan/MoS<sub>2</sub>/GO membrane for catalytic degradation of organic contaminants, *Environ. Technol. Innov.*, 2023, **32**, 103410, DOI: [10.1016/J.ETI.2023.103410](https://doi.org/10.1016/J.ETI.2023.103410).
- 91 M. Hosseini, M. Sarafbidabad, A. Fakhri, Z. NoorMohammadi and S. Tahami, Preparation and characterization of MnS<sub>2</sub>/chitosan-sodium alginate and calcium alginate nanocomposites for degradation of analgesic drug: Photocorrosion, mechanical, antimicrobial and antioxidant properties studies, *Int. J. Biol. Macromol.*, 2018, **118**, 1494–1500, DOI: [10.1016/J.IJBIOMAC.2018.06.176](https://doi.org/10.1016/J.IJBIOMAC.2018.06.176).
- 92 J. W. Tu, Y. Li, L. Chen and W. Miao, Iron-loading N and S heteroatom doped porous carbon derived from chitosan and CdS-Tetrahymena thermophila for peroxymonosulfate activation, *Int. J. Biol. Macromol.*, 2023, **253**, 127347, DOI: [10.1016/J.IJBIOMAC.2023.127347](https://doi.org/10.1016/J.IJBIOMAC.2023.127347).
- 93 T. Xiang, D. Zhong, Y. Zhou, Y. Xu, W. Li, D. Tang, Y. Yang, C. Fan and J. Chen, Efficient degradation of organic pollutants by ozone oxidation catalyzed by chitosan-derived N-doped carbon and MnFe<sub>2</sub>O<sub>4</sub> co-doped CuS, *Int. J. Biol. Macromol.*, 2025, **319**, 145671, DOI: [10.1016/J.IJBIOMAC.2025.145671](https://doi.org/10.1016/J.IJBIOMAC.2025.145671).
- 94 H. Peng, L. Wang and X. Zheng, Efficient adsorption-photodegradation activity of MoS<sub>2</sub> coupling with S,N-codoped porous biochar derived from chitosan, *J. Water Proc. Eng.*, 2023, **51**, 103426, DOI: [10.1016/J.JWPE.2022.103426](https://doi.org/10.1016/J.JWPE.2022.103426).
- 95 R. Jiang, D. Zhong, Y. Xu, Y. He, J. Zhang and P. Liao, Chitosan-derived N-doped carbon supported Cu/Fe co-doped MoS<sub>2</sub> nanoparticles as peroxymonosulfate activator for efficient dyes degradation, *Int. J. Biol. Macromol.*, 2024, **278**, 134352, DOI: [10.1016/J.IJBIOMAC.2024.134352](https://doi.org/10.1016/J.IJBIOMAC.2024.134352).
- 96 X. He, J. Gan, A. Fakhri, B. F. Dizaji, M. H. Azarbaijan and M. Hosseini, Preparation of ceric oxide and cobalt sulfide-ceric oxide/cellulose-chitosan nanocomposites as a novel catalyst for efficient photocatalysis and antimicrobial study, *Int. J. Biol. Macromol.*, 2020, **143**, 952–957, DOI: [10.1016/J.IJBIOMAC.2019.09.155](https://doi.org/10.1016/J.IJBIOMAC.2019.09.155).
- 97 I. Raeisi and Z. Yousefpour, Dual-responsive drug carrier based on zeolitic imidazolate framework-8 incorporated into gold nanoparticles/chitosan/copper sulfide for controlled drug delivery, *J. Drug Deliv. Sci. Technol.*, 2024, **98**, 105883, DOI: [10.1016/J.JDDST.2024.105883](https://doi.org/10.1016/J.JDDST.2024.105883).
- 98 S. Zhang, Saeeda, A. Khan, N. Ali, S. Malik, H. Khan, N. Ali, H. M. N. Iqbal and M. Bilal, Designing, characterization, and evaluation of chitosan-zinc selenide nanoparticles for visible-light-induced degradation of tartrazine and sunset yellow dyes, *Environ. Res.*, 2022, **213**, 113722, DOI: [10.1016/J.ENVRES.2022.113722](https://doi.org/10.1016/J.ENVRES.2022.113722).
- 99 K. Kumari, S. R. Mishra, V. Gadore, N. S. Moyon and M. Ahmaruzzaman, Efficient Visible-Light Photocatalysis Using Fe-Doped SnO<sub>2</sub>/Chitosan Composite for Organic Pollutant Degradation: Mechanisms, Reusability, and Sustainability, *J. Inorg. Organomet. Polym. Mater.*, 2025, **1–24**, DOI: [10.1007/S10904-025-03700-Z](https://doi.org/10.1007/S10904-025-03700-Z).
- 100 D. E. Al Momani, F. Arshad and L. Zou, Chitosan/MoS<sub>2</sub>/Go Membrane Reactor for Catalytic Degradation of Organic Contaminants, 2023, DOI: [10.2139/SSRN.4480914](https://doi.org/10.2139/SSRN.4480914).
- 101 E. Kusri, L. D. Wilson, K. M. Padmosoedarso, D. P. Mawarni, M. Sufyan and A. Usman, Synthesis of Chitosan Capped Zinc Sulphide Nanoparticle Composites as an Antibacterial Agent for Liquid Handwash Disinfectant Applications, *J. Compos. Sci.*, 2023, **7**, 52, DOI: [10.3390/JCS7020052/S1](https://doi.org/10.3390/JCS7020052/S1).
- 102 Y. Han, J. Tao, A. Khan, A. Khan, N. Ali, S. Malik, C. Yu, Y. Yang, T. Jesionowski and M. Bilal, Development of reusable chitosan-supported nickel sulfide microspheres for environmentally friendlier and efficient bio-sorptive decontamination of mercury toxicant, *Environ. Sci. Pollut. Res.*, 2023, **30**, 47077–47089, DOI: [10.1007/S11356-022-24563-8](https://doi.org/10.1007/S11356-022-24563-8).
- 103 S. Bahri, A. Homaei and E. Mosaddegh, Zinc sulfide-chitosan hybrid nanoparticles as a robust surface for immobilization of Sillago sihama  $\alpha$ -amylase, *Colloids Surf., B*, 2022, **218**, 112754, DOI: [10.1016/J.COLSURFB.2022.112754](https://doi.org/10.1016/J.COLSURFB.2022.112754).
- 104 M. Xiao, R. Jiang, Z. Xu, Q. Wang, Y. Fu, S. Jiang, Y. Long and H. Zhu, Floatable and magnetic MoS<sub>2</sub>/NiFe<sub>2</sub>O<sub>4</sub>/chitosan nanocomposite integrated melamine sponges with hybrid photothermal and photocatalytic enhancement for pollutant removal, *Int. J. Biol. Macromol.*, 2025, **291**, 138965, DOI: [10.1016/J.IJBIOMAC.2024.138965](https://doi.org/10.1016/J.IJBIOMAC.2024.138965).
- 105 B. Janani, R. Balakrishnaraja, A. M. Elgorban, A. H. Bahkali, R. S. Varma, A. Syed and S. S. Khan, Eco-friendly cubic-ZnS coupled Cu<sub>7</sub>S<sub>4</sub> spines on chitosan matrix: Unravelling defect-engineered nanoplatfor for the photodegradation of p-chlorophenol, *J. Environ. Manage.*, 2023, **326**, 116615, DOI: [10.1016/J.JENVMAN.2022.116615](https://doi.org/10.1016/J.JENVMAN.2022.116615).
- 106 P. Sirajudheen, S. Vigneshwaran, N. Thomas, M. Selvaraj, K. Venkatesan and C. M. Park, Fabrication of MoS<sub>2</sub> restrained magnetic chitosan polysaccharide composite for the photocatalytic degradation of organic dyes, *Carbohydr. Polym.*, 2024, **335**, 122071, DOI: [10.1016/J.CARBPOL.2024.122071](https://doi.org/10.1016/J.CARBPOL.2024.122071).

